

See discussions, stats, and author profiles for this publication at: <https://www.researchgate.net/publication/260916280>

ChemInform Abstract: Highly Efficient Direct Aerobic Oxidative Esterification of Cinnamyl Alcohol with Alkyl Alcohols Catalyzed by Gold Nanoparticles Incarcerated in a Nanoporous P...

ARTICLE *in* CHEMISTRY - A EUROPEAN JOURNAL · SEPTEMBER 2014

Impact Factor: 5.73 · DOI: 10.1002/chem.201303880 · Source: PubMed

CITATIONS

5

READS

197

3 AUTHORS, INCLUDING:



[Antonio Buonerba](#)

Università degli Studi di Salerno

42 PUBLICATIONS 85 CITATIONS

[SEE PROFILE](#)



[Annarita Noschese](#)

Università degli Studi di Salerno

6 PUBLICATIONS 5 CITATIONS

[SEE PROFILE](#)

Nanoporous Catalysis

Highly Efficient Direct Aerobic Oxidative Esterification of Cinnamyl Alcohol with Alkyl Alcohols Catalysed by Gold Nanoparticles Incarcerated in a Nanoporous Polymer Matrix: A Tool for Investigating the Role of the Polymer Host

Antonio Buonerba, Annarita Noschese, and Alfonso Grassi^{*[a]}

Dedicated to Professor Adolfo Zambelli on the occasion of his 80th birthday

Abstract: The selective aerobic oxidation of cinnamyl alcohol to cinnamaldehyde, as well as direct oxidative esterification of this alcohol with primary and secondary aliphatic alcohols, were achieved with high chemoselectivity by using gold nanoparticles supported in a nanoporous semicrystalline multi-block copolymer matrix, which consisted of syndiotactic polystyrene-*co*-*cis*-1,4-polybutadiene. The cascade reaction that leads to the alkyl cinnamates occurs through two oxidation steps: the selective oxidation of cinnamyl alcohol to cinnamaldehyde, followed by oxidation of the hemiacetal that results from the base-catalysed reaction of cinnamaldehyde with an aliphatic alcohol. The rate constants for the two steps were evaluated in the temperature range 10–45 °C. The cinnamyl alcohol oxidation is faster than the oxidative esterification of cinnamaldehyde with methanol, etha-

nol, 2-propanol, 1-butanol, 1-hexanol or 1-octanol. The rate constants of the latter reaction are pseudo-zero order with respect to the aliphatic alcohol and decrease as the bulkiness of the alcohol is increased. The activation energy (E_a) for the two oxidation steps was calculated for esterification of cinnamyl alcohol with 1-butanol ($E_a = 57.8 \pm 11.5$ and 62.7 ± 16.7 kJ mol⁻¹ for the first and second step, respectively). The oxidative esterification of cinnamyl alcohol with 2-phenylethanol follows pseudo-first-order kinetics with respect to 2-phenylethanol and is faster than observed for other alcohols because of fast diffusion of the aromatic alcohol in the crystalline phase of the support. The kinetic investigation allowed us to assess the role of the polymer support in the determination of both high activity and selectivity in the title reaction.

Introduction

Cinnamic aldehydes, acids and esters are widely distributed in nature and constitute a class of compounds with a broad spectrum of pharmaceutical activities, such as anti-inflammatory, anticonvulsant, antifungal, analgesic and antihypertensive effects. Moreover, they also find application in the perfumery and cosmetics industries.^[1] For example, methyl caffeate is reported to exhibit antitumour activity against Sarcoma 180, as well as antimicrobial activity.^[2] Methoxy-substituted cinnamates play an important role in the control of inflammatory diseases.^[3] Long-chain cinnamic esters are well-known as sunscreen agents and are ideally suited for cosmetic applications because they are not skin irritants and prevent the drying effect of

wind.^[4] Cinnamic esters are obtained from various plant sources or, alternatively, synthesised when the naturally occurring compounds are not cheap and/or commercially available.

The conventional synthesis of esters from alcohols, when the latter are naturally occurring and/or cheaper than the respective acid, involves a two-step reaction: oxidation of the alcohol to the corresponding acid, followed by condensation with an alcohol.^[5] The latter step is an equilibrium reaction that requires the elimination of water by co-distillation or trapping with specific reagents to move the equilibrium toward the expected reaction products. Alternatively, activated forms of the carboxylic acids—the acyl halides—must be used, which leads to irreversible reactions. The latter synthetic approach is, of course, more convenient but the formation of toxic wastes (hydrochloric acid and/or other by-products) is undesirable from the viewpoint of sustainable chemistry. Because of the industrial interest given to alkyl cinnamates, efforts have been made to optimise the synthesis under more convenient and environmentally friendly conditions.

The synthesis of methyl, ethyl, 1-propyl, 1-butyl or longer alkyl chain cinnamates has recently been reported by using heteropolyacid catalysts and microwave irradiation.^[6] Good conversion and selectivity were generally observed with strong irradiation power (e.g. 130 mA, 410 W). For example, in the

[a] Dr. A. Buonerba, Dr. A. Noschese, Prof. A. Grassi

Dipartimento di Chimica e Biologia and
NANOMATES Research Centre for NANOMaterials and
nanoTEchnology at Salerno University

Università degli Studi di Salerno

Via Giovanni Paolo II

84084 Fisciano (SA) (Italy)

Fax: (+39) 089969824

E-mail: agrassi@unisa.it

 Supporting information for this article is available on the WWW under
<http://dx.doi.org/10.1002/chem.201303880>.

case of butyl cinnamate, a cinnamic acid conversion of 92.8 mol% was obtained after irradiation of the reaction mixture for 3 h, catalysed by $\text{SO}_4^{2-}\text{-La}_2\text{O}_3\text{-ZrO}_2\text{-HZSM-5}$. Although this method seems feasible, the increase of the alkyl cinnamate output and the use of this technology in industry is not straightforward.

Supported gold nanoparticles (AuNPs) are emerging as a powerful tool in catalysis. AuNPs were found to be active in several chemical transformations,^[7] which include the oxidation of carbon monoxide,^[8] alkanes,^[9] alcohols,^[10] polyols and aldehydes, the epoxidation of alkenes,^[11] the reduction of α,β -unsaturated carbonyl compounds^[12] and nitroarenes,^[13] as well as the direct synthesis of hydrogen peroxide^[14] and acetylene hydrochlorination.^[15] Probably one of the most interesting application of AuNPs is in tandem catalysis, in which cascade reactions are carried out in a single reactor, thus the efficiency of the chemical synthesis, in terms of energy consumption and waste formation, is increased. The efficient synthesis of esters^[16] and amides^[17] has been successfully achieved by one-pot aerobic oxidative esterification of alcohols or by oxidative coupling of alcohols with amines, respectively. A variety of materials have been explored to efficiently support the AuNPs, such as carbon^[7e] or inorganic oxides, such as alumina, titania^[7j] and ceria,^[18] or polymers [e.g. poly(vinyl alcohol),^[19] poly(*N*-vinyl-2-pyrrolidone)],^[20] dendrimers (poly(amido amine); PAMAM),^[21] cationic ion-exchange resins,^[22] and random copolymers of styrene and its *para*-substituted derivatives.^[23]

Oxidation of cinnamyl alcohol (CA) to cinnamaldehyde has generally been carried out as a benchmark test for the performance of AuNP-supported catalysts in the selective oxidation of alcohols to aldehydes. In principle, a complex mixture of products can be obtained as a result of oxidation, dehydrogenation, hydrogenolysis and decarbonylation pathways (Scheme 1).^[24] Few reports deal with the oxidative esterification

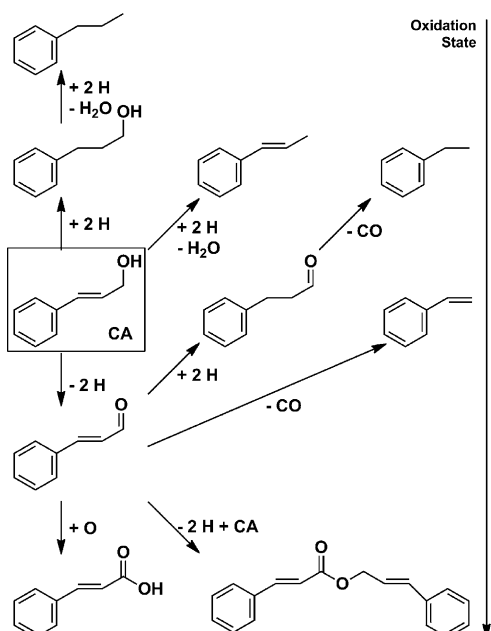
of CA and these are mainly focused on methyl cinnamate synthesis.^[24] Recently we reported the efficient and selective aerobic oxidation of alcohols catalysed by AuNPs^[25] incarcerated in a nanoporous semi-crystalline polymer matrix that consisted of multi-block copolymers^[26] of syndiotactic polystyrene-*co*-1,4-*cis*-polybutadiene (AuNPs-sPSB). Primary and secondary benzyl or allyl alcohols were readily oxidised to the corresponding aldehydes, whereas alkyl alcohols were not oxidised at all under the same experimental conditions. Although primary and secondary alkyl alcohols are known to be less reactive in this reaction, the observed selectivity appeared unprecedented, as did the specific properties of the polymeric support employed.

These results prompted us to investigate the oxidation and oxidative esterification of CA catalysed by AuNPs-sPSB; we also tried to obtain information on the reaction mechanism.

Results and Discussion

Synthesis of the AuNPs-sPSB catalyst

The AuNPs-sPSB catalyst (gold content = 2% w/w) was synthesised by the method previously reported,^[25] by using the multi-block copolymer sPSB with a high concentration in styrene (93% w/w) to enhance the selectivity properties of the polymeric support and keep the butadiene concentration high enough to yield good swelling of the polymer matrix. The powder wide-angle X-ray diffraction (WAXD) pattern of the AuNPs-sPSB catalyst is shown in Figure 1. The region 4–30° provides information about the crystalline phase of the polymeric support,^[27] whereas the peak at 38°, due to the <111> plane of the fcc crystal lattice of gold, allows evaluation of the average dimension of the nanoparticles from the Scherrer equation.^[28] The as-synthesised catalyst presents the syndiotactic polystyrene (sPS) polymer phase in the δ -crystalline form and comprises THF molecules clathrated in the nanopores of



Scheme 1. Reaction pathways for oxidation/reduction of cinnamyl alcohol.

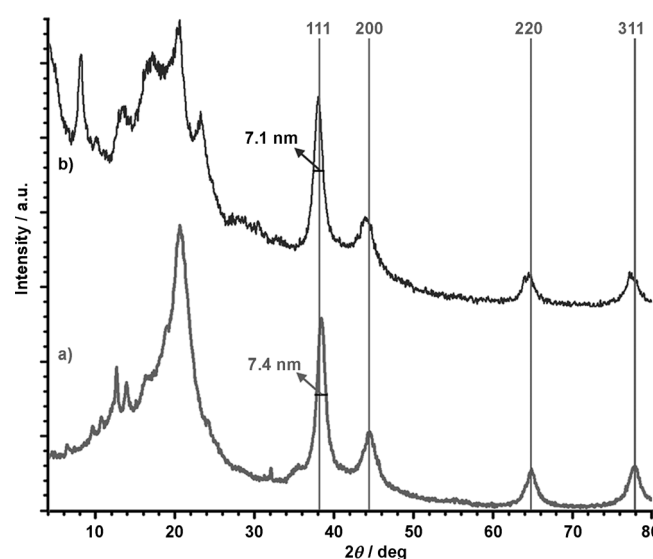


Figure 1. WAXD patterns of the AuNPs-sPSB catalyst after thermal treatment at 170 °C for a) 5 h and b) after a catalytic cycle.

the crystalline phase^[27] and AuNPs with an average dimension of about 4.4 nm (Figures S1 and S2 in the Supporting Information). The annealing of AuNPs-sPSB at 170 °C for 5 h to activate the AuNPs^[25] converts the crystalline phase of the polymer matrix from δ to β form and produces a slight increase of the AuNPs dimension to 7.4 nm (Figure 1a).

The transmission electron microscopy (TEM) confirmed the average diameter of the AuNPs and reveals their optimal dispersion in the polymer matrix (Figure 2). From inspection of the selected-area electron diffraction (SAED) micrograph (Figure 2c; Figure S3 in the Supporting Information) it is possible to recognise two patterns: the diffuse halo attributed to the unoriented AuNPs and the spotted pattern due to the sPS crystalline phase. Attempts to obtain a narrower distribution of the AuNPs by variation of the experimental conditions of the synthetic process were unfruitful. To obtain smaller AuNPs, gold precursors different from HAuCl₄ are likely necessary.

Oxidation of CA to cinnamaldehyde catalysed by AuNPs-sPSB

The aerobic oxidation of CA catalysed by AuNPs-sPSB was preliminarily investigated under the experimental conditions previously reported [35 °C, 1:1 v/v water/chloroform, P_{O_2} =1 bar, KOH (1 equiv)].^[25] After 2 h, the alcohol conversion is 97% with a selectivity of 97% for cinnamaldehyde (Table 1, entry 1; Figure S5 in the Supporting Information). With KOH (6 equiv), the

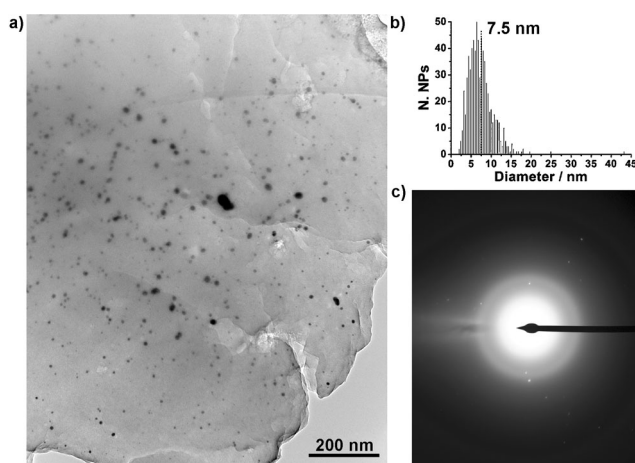


Figure 2. a) TEM micrograph of annealed AuNPs-sPSB catalyst (170 °C for 5 h), b) the AuNPs size distribution, c) SAED micrograph.

CA oxidation is quantitative after 1.5 h with a selectivity of 99% (Table 1, entry 2; Figure 3), whereas use of KOH (20 equiv) led to the same result after 4 h (Table 1, entry 3). When the temperature was decreased to 10 or 25 °C, longer reaction times were necessary to obtain high conversion and selectivity to cinnamaldehyde (Table 1, entries 4 and 5; Figure 3). The increase of the reaction temperature to 45 °C shortens the reaction time and leaves selectivity totally unaffected (99%; Table 1, entry 6). The kinetic plots of CA oxidation to cinnamal-

Table 1. Aerobic oxidation of cinnamyl alcohol catalysed by AuNPs-sPSB.

Entry ^[a]	T [°C]	KOH/CA	Solvent ^[b]	t [h]	Conversion ^[c,d] [%]	Products	Yield ^[d] [%]	Selectivity ^[d] [%]
1	35	1	H ₂ O/CHCl ₃	2	97	cinnamaldehyde 3-phenyl-1-propanol	94 3.0	97 3.0
2	35	6	H ₂ O/CHCl ₃	1.5	>99	cinnamaldehyde 3-phenyl-1-propanol	98 1.5	99 1.0
3	35	20	H ₂ O/CHCl ₃	4	>99	cinnamaldehyde 3-phenyl-1-propanol	92 1.9	92 1.9
4	10	6	H ₂ O/CHCl ₃	8	>99	cinnamaldehyde 3-phenyl-1-propanol	95 5.0	95 5.0
5	25	6	H ₂ O/CHCl ₃	5	98	cinnamaldehyde 3-phenyl-1-propanol	94 4.0	96 4.0
6	45	6	H ₂ O/CHCl ₃	0.75	97	cinnamaldehyde 3-phenyl-1-propanol	96 1.3	99 1.0
7	35	6	H ₂ O/ethyl acetate	24	20	cinnamaldehyde 3-phenyl-1-propanol	18 2.0	91 9.0
8	35	6	H ₂ O/2-butanone	8	44	7-phenylhepta-4,6-dien-3-one cinnamaldehyde 3-phenyl-1-propanol	31 3.6 3.4	69 8.7 8.3
9	35	6	H ₂ O/cyclohexanone	6	56	cinnamaldehyde 3-phenyl-1-propanol	52 4.0	93 7.0
10	35	6	H ₂ O/toluene	3	90	cinnamaldehyde 3-phenyl-1-propanol	84 0.9	93 1.4

[a] Reaction conditions: CA (0.51 mmol), AuNPs-sPSB (200 mg, Au=2% w/w), O₂ (1 atm), anisole as an internal standard (0.51 mmol). [b] v/v=1:1, total volume=6 mL. [c] Conversion of CA. [d] Determined by GC-MS analysis.

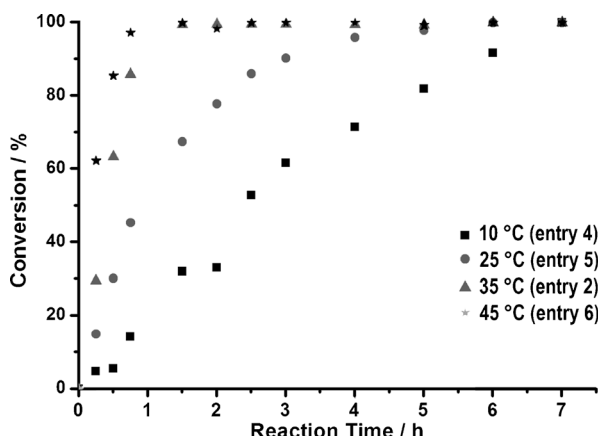


Figure 3. Cinnamyl alcohol oxidation to cinnamaldehyde in the temperature range 10–45 °C.

dehyde in the temperature range 10–45 °C are displayed in Figure 3. The rate constants, calculated assuming first-order kinetics with respect to CA, are in the range $k=1.08 \times 10^{-4} \pm 7.1 \times 10^{-6}$ – $1.3 \times 10^{-3} \pm 1.3 \times 10^{-4}$ s $^{-1}$. The corresponding Arrhenius plot gives an activation energy (E_a) value of 57.8 ± 11.5 kJ mol $^{-1}$ (Figure S14 in the Supporting Information).

Alternative solvents to chloroform, to be mixed with water for efficient oxidation catalysis, were investigated. Ethyl acetate produced a dramatic decrease in the catalytic activity (Table 1, entry 7), probably a result of the reduced swelling of the crystalline polymer support. Reaction in 2-butanone led to the formation of 7-phenylhepta-4,6-dien-3-one—the result of the base-catalysed aldol reaction of 2-butanone with cinnamaldehyde—in low yields (Table 1, entry 8). Use of cyclohexanone gave a CA conversion of 56% with a selectivity of 93% for cinnamaldehyde in 6 h (Table 1, entry 9), whereas toluene produced an alcohol conversion of 90% with a selectivity of 93% for cinnamaldehyde (Table 1, entry 10). The aromatic solvent efficiently swells the crystalline polymer support to ensure good accessibility of the substrates to the AuNPs incarcerated in the polymer phase. Nonetheless, chloroform remained the solvent of choice.

The peculiar properties of chloroform as the reaction solvent were investigated next. The diffuse-reflectance FTIR (DRIFT) analysis combined with WAXD investigation of the catalyst soon after an oxidation run in water/chloroform showed that the polymer support is crystalline in the nanoporous ϵ -crystalline phase of sPS (Figure 1 b; Figure S4 in the Supporting Information) and the crystallisation process that leads to this crystalline polystyrenic phase is unexpectedly fast under the catalytic conditions. We have previously shown that the efficient aerobic oxidation of both benzyl alcohol and 1-phenylethanol catalysed by AuNPs-sPSB in chloroform/water follows first-order kinetics with respect to the alcohol,^[25] this result is similar to that observed for alcohol oxidation catalysed by AuNPs supported on metal oxides. We attributed this kinetic behaviour to the fast diffusion of the substrates into the nanochannels of the ϵ -crystalline polymer phase; in fact, zero-order kinetics with respect to alcohol were observed with AuNPs incar-

cerated in a cross-linked atactic polystyrene matrix because of slow diffusion of the reagent through the amorphous polymer phase.^[10f] Our findings for CA oxidation confirmed this hypothesis. Alcohols with aromatic substituents behave similarly to aromatic compounds (e.g. toluene, 4-nitrophenol, azobenzene, benzaldehyde), which are known to establish strong interactions with the cavities of the ϵ crystalline form and lead to well-characterized co-crystalline compounds.^[27] Moreover, it was recently demonstrated that sPS clathrates in chloroform undergo rapid guest-exchange processes, which promotes fast diffusion of the guest molecules in the nanochannels of the ϵ -crystalline form.^[29] Thus, chloroform plays the following peculiar roles: 1) swelling of the polymer matrix; 2) in situ formation of the crystalline nanoporous ϵ phase; 3) fast diffusion of the reagents through the nanochannels of the polymer support. From a sustainable point of view, chloroform is an unpleasant solvent. However in these oxidation reactions it is used in very small amounts, for polymer swelling and to ensure biphasic catalysis. In principle, the reagents and products can be extracted from the organic layer by treatment with immiscible polar solvents and the AuNPs-sPSB catalyst, swollen in chloroform, can be reused without the requirement for additional chlorinated solvents. Actually, it was previously shown that the AuNPs-sPSB catalyst can be used at least six times without observation of a decrease in the activity or selectivity of the alcohol oxidation.^[25]

It is also noteworthy that 3-phenyl-1-propanol was found as a minor product in all of the CA oxidation runs. This compound could result from hydrogen addition to the olefinic carbon–carbon double bond of CA (Scheme 1). This piece of experimental evidence supports the formation of a Au–H^[23b] intermediate species and the possibility of intermolecular hydrogen borrowing^[30] or transfer^[31] from the alcohol to be oxidised to other substrates.

Figure 3 displays the kinetic profiles of the CA oxidation in the temperature range 10–45 °C. As previously observed for the oxidation of benzyl alcohol catalysed by AuNPs-sPSB,^[25] the reaction exhibits pseudo-first-order kinetics with respect to the CA. This confirms that the access of CA to the AuNPs is not controlled by a diffusive process through the amorphous phase of the polymer, rather through the nanoporous crystalline phase. The rate constants for the CA oxidation were measured in the temperature range 10–45 °C and the corresponding Arrhenius plot (Figure S14 in the Supporting Information) gives $E_a=57.8 \pm 11.5$ kJ mol $^{-1}$ for this reaction. This value is in good agreement with that found for the oxidation of *p*-methyl benzyl alcohol catalysed by AuNPs-Ce/O₂^[18b] and higher than that for oxidation of activated *p*-hydroxybenzyl alcohol catalysed by AuNPs incarcerated in poly(*N*-vinyl-2-pyrrolidone).^[20b] It is notable that in the both cases a specific activating role of the support was claimed,^[10c, 18b, 20] whereas the AuNPs-sPSB consists only of a hydrocarbon polymer support.

Oxidative esterification of CA with aliphatic alcohols

Recently, the reaction mechanism of aerobic oxidation of alcohols and the oxidative esterification of alcohols catalysed by

AuNPs have been extensively investigated.^[10,16,18b,23,24,32] The reaction pathway of the latter includes alcohol oxidation to give aldehyde, which in turn reacts with the same or another alcohol molecule to yield the corresponding hemiacetal, which is finally oxidised to the ester. The reaction requires a strong Brønsted base as a co-catalyst, especially when the AuNPs are supported/incarcerated in organic polymers. The AuNPs-sPSB catalyst reached the highest activity for benzyl alcohol oxidation with a KOH/alcohol molar ratio of 1; activity decreases at higher molar ratio.^[25] Oxidative esterification of CA with 1-butanol was, thus, preliminarily carried out with variance of the KOH concentration to search for the best reaction conditions; the main results are given in Table 2.

When the concentration of KOH was increased from 1 to 12 equivalents (Table 2, entries 1–4; Figures S6 and S7 in the Supporting Information), butyl cinnamate reached the highest yield (48%) at KOH/CA molar ratio of 6 after 3 h (Table 2, entry 3; Figure S7 in the Supporting Information), whereas the

CA conversion was quantitative after 1.5 h. Further increase of KOH (12 equiv) resulted in a decrease of catalytic activity, which confirmed that the concentration of the base is critical to the catalytic performance of the polymer-incarcerated AuNPs. To date the role of base is not completely understood. In oxidation reactions catalysed by polymer-incarcerated AuNPs, the hydroxyl species, coordinated to the nanoparticle surface, would promote deprotonation of the alcohol and favour its coordination to the gold nanoparticle surface, followed by β-hydrogen transfer to gold. The results we obtained for the CA oxidative esterification suggest a more complex role of this co-catalyst. The oxidative esterification of CA with different primary and secondary alcohols, namely methanol, ethanol, 2-propanol, 1-hexanol, 1-octanol and 2-phenylethanol was carried out by using KOH (6 equiv) at 35 °C to gain information on the selectivity of the nanoporous host–polymer matrix.

Under these mild conditions, esterification of CA with short alkyl chain alcohols (methanol and ethanol) proceeds rapidly

to afford methyl cinnamate (90%, 4 h; Table 2, entry 5; Figure S8 in the Supporting Information) and ethyl cinnamate (94%, 5 h; Table 2, entry 6; Figure 4a) in high yields, whereas the esterification of bulkier alcohols, 2-propanol, 1-hexanol and 1-octanol (Table 2, entries 7–9) is slower. These findings suggest that the bulkiness of the alkyl chain is a critical parameter in the diffusion toward the gold catalyst through the polymer support. Surprisingly, oxidative esterification of 2-phenylethanol is particularly efficient (Table 2, entry 20; Figure 4b), probably a result of the high affinity of this aromatic alcohol with the polystyrene matrix. It is well known that aromatic compounds establish strong interactions with the cavities of the δ- and ε-crystalline forms of sPS.^[27] The kinetic profiles of the reactions of CA with ethanol and 2-phenylethanol are compared (Figure 4). CA is readily oxidised to cinnamaldehyde after 1.5–2 h, then the reaction of the aldehyde with the alkyl alcohol begins and leads to the hemiacetal, which is definitively oxidised to the alkyl cinnamate. The reaction with ethanol is quantitative after 5 h, whereas that of 2-phenylethanol reaches a conversion of 44% of cinnamyl

Table 2. Synthesis of alkyl cinnamates by aerobic oxidative esterification of cinnamyl alcohol and alkyl alcohols.

Entry ^[a]	Alkyl alcohol	KOH/CA	t [h]	Conversion ^[b,c] [%]	Products	Yield ^[c] [%]
1	1-butanol	1	3	>99	butyl cinnamate cinnamaldehyde 3-phenyl-1-propanol	29 69 2
2	1-butanol	3	3	>99	butyl cinnamate cinnamaldehyde 3-phenyl-1-propanol	28 69 3.0
3	1-butanol	6	3	>99	butyl cinnamate cinnamaldehyde 3-phenyl-1-propanol	48 46 6.0
4	1-butanol	12	3	>99	butyl cinnamate cinnamaldehyde 3-phenyl-1-propanol	44 48 8.0
5	methanol	6	4	>99	methyl cinnamate cinnamaldehyde 3-phenyl-1-propanol	90 8.1 1.9
6	ethanol	6	5	>99	ethyl cinnamate cinnamaldehyde 3-phenyl-1-propanol	94 0 6.0
7	2-propanol	6	5	>99	isopropyl cinnamate cinnamaldehyde 3-phenyl-1-propanol	9.2 86 4.8
8	1-hexanol	6	5	>99	hexyl cinnamate cinnamaldehyde 3-phenyl-1-propanol	12 85 3.0
9	1-octanol	6	5	>99	octyl cinnamate cinnamaldehyde 3-phenyl-1-propanol	11 86 3.0
10	2-phenylethanol	6	5	>99	2-phenylethyl cinnamate cinnamaldehyde 3-phenyl-1-propanol	44 50 2.0

[a] Reaction conditions: CA (0.51 mmol), AuNPs-sPSB (200 mg, Au=2% w/w), alkyl alcohol (5.1 mmol), 35 °C, O₂ (1 atm), H₂O/CHCl₃ (v/v = 1:1, total volume = 6 mL), anisole as an internal standard (0.51 mmol). [b] Conversion of CA. [c] Determined by GC-MS analysis.

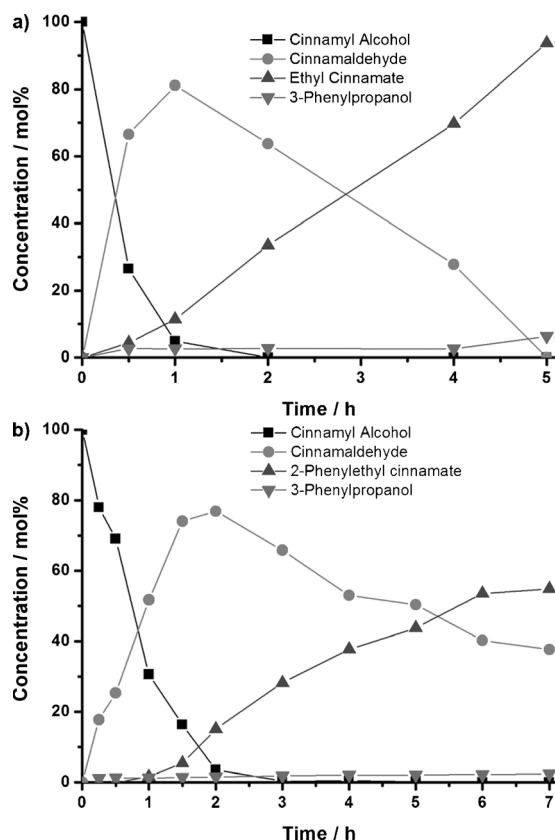


Figure 4. Kinetic profiles of the oxidative esterification of cinnamyl alcohol with: a) ethanol (Table 2, entry 6); b) 2-phenylethanol (Table 2, entry 10).

ester in the same time. The rate constants for this reaction with the quoted alkyl alcohols are given in Table 3. The reaction proceeds faster with short-chain aliphatic alcohols, whereas small rate constants were measured for 2-propanol, 1-hexanol and 1-octanol. Moreover, the kinetics for the oxidative esterification of cinnamaldehyde is pseudo-zero order for aliphatic alcohols and pseudo-first order for 2-phenylethanol (Table 3), which confirms the different mechanism for access of the oxidation substrates to the catalytic sites.

Table 3. Rate constants for the oxidative esterification of cinnamaldehyde with alkyl alcohols. ^[a]			
Entry	Alkyl alcohol ^[b,c]	k_{obs} [mol L ⁻¹ s ⁻¹]	Evaluated from Table 2, entry x
1	methanol	4.63×10^{-6}	5
2	ethanol	4.65×10^{-6}	6
3	1-butanol	4.93×10^{-6}	3
4	2-propanol	5.38×10^{-7}	7
5	1-hexanol	6.12×10^{-7}	8
6	1-octanol	1.14×10^{-6}	9
7	2-phenylethanol ^[d]	4.35×10^{-5} s ⁻¹	10

[a] Evaluated from the second reaction step of the cinnamyl alcohol oxidation. [b] Reaction conditions: cinnamyl alcohol (0.51 mmol), AuNPs-sPSB (200 mg, Au=2% w/w), alkyl alcohol (5.1 mmol), KOH (3.06 mmol), 35 °C, O₂ (1 atm), H₂O/CHCl₃ (v/v=1:1, total volume=6 mL), anisole as an internal standard (0.51 mmol). [c] Pseudo-zero-order reaction. [d] Pseudo-first-order reaction.

Notably, the one-pot synthesis of alkyl cinnamates catalysed by AuNPs-sPSB exhibits one of the highest reaction rates and selectivities, under mild conditions, reported to date in the literature.^[16] The turnover frequency (TOF) calculated for the first oxidation step at 35 °C is 21.2 h⁻¹, whereas TOF=5.6 h⁻¹ for the esterification of CA to methyl cinnamate (Table 2, entry 5). To the best of our knowledge the highest TOF reported for the oxidative esterification of CA to methyl cinnamate is 7.4 h⁻¹ at 100 °C.^[16b] In the oxidative esterification of CA with alkyl alcohols catalysed by AuNPs-sPSB we found that the oxidation of CA to cinnamaldehyde proceeds faster than the oxidative coupling of the latter with alkyl alcohols.

We investigated the esterification of cinnamaldehyde with 1-butanol catalysed by AuNPs-sPSB to shed light on the kinetics of this cascade reaction in the temperature range 10–45 °C. To avoid overlap of the kinetic curves due to the two consecutive reactions, esterification of cinnamaldehyde with 1-butanol was also performed independently (Table 4 and Figure 5). The rate

Table 4. Esterification of cinnamaldehyde with 1-butanol.

Entry ^[a]	T [°C]	t [h]	Yield ^[b] [%]	Selectivity ^[b] [%]
1	10	6	6.7	>99
2	25	7	12	>99
3	35	6	>99	>99
4	45	6	89	>99

[a] Reaction conditions: cinnamaldehyde (0.51 mmol), 1-butanol (5.1 mmol), AuNPs-sPSB (200 mg, Au=2% w/w), O₂ (1 atm), H₂O/CHCl₃ (v/v=1:1, total volume=6 mL), KOH (3.06 mmol, 6 equiv); anisole as an internal standard (0.51 mmol). [b] Determined by GC-MS analysis.

constant (k) of 4.09×10^{-6} mol L⁻¹ s⁻¹ calculated for the latter reaction at 35 °C (Table 4, entry 3; Figure S9 in the Supporting Information) well compares to that found for the second step of the oxidative esterification of cinnamyl alcohol with 1-butanol ($k=4.93 \times 10^{-6}$ mol L⁻¹ s⁻¹; Table 3, entry 3; Figure S7 in the Supporting Information). The Arrhenius plot gives $E_a=62.7 \pm 16.7$ kJ mol⁻¹ (Figure S15 in the Supporting Information) for this oxidation reaction.

Notably, 3-phenyl-1-propanol, found in traces in CA oxidation (Tables 1 and 2), is not observed in the oxidative esterification of cinnamaldehyde with 1-butanol, which suggests that this compound is formed in the first reaction step.

Oxidative esterification of *p*-substituted cinnamyl alcohols

Alkyl cinnamates with hydroxy, halide or alkoxy substituents on the aromatic ring are important chemicals in the pharmaceutical and cosmetic industries.^[1] To test the validity of the synthetic protocol described, oxidative esterification of *p*-meth-

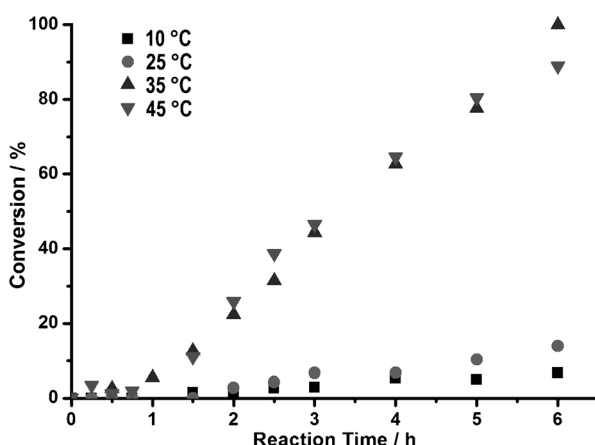


Figure 5. Oxidative esterification of cinnamaldehyde with 1-butanol in the temperature range 10–45 °C (Table 5).

oxy- and *p*-chloro- cinnamyl alcohol with methanol and 1-butanol was investigated under the experimental conditions of the CA oxidation (Table 5). Quantitative conversion for the oxidation of *p*-substituted cinnamyl alcohols to aldehydes was achieved after 2 h. However, *p*-methoxy cinnamyl alcohol (Table 5, entries 1 and 2; Figures S10 and S11 in the Supporting Information) is oxidised faster than *p*-chlorocinnamyl alcohol (Table 5,

entries 3 and 4; Figures S12 and S13 in the Supporting Information), likely as a result of the activating effect of the electron-releasing substituent. This supports the formation of an ionic intermediate species with a positive charge on the carbonyl carbon atom to be oxidised.^[18b] The overall oxidative esterification of *p*-methoxy- and *p*-chloro-cinnamyl alcohol with methanol and 1-butanol is slower than the analogous reaction of CA. Also, in this case, the reaction is faster for methanol and seems to be activated by electron-withdrawing groups, which increase the electrophilicity of the carbonyl carbon atom of the intermediate aldehyde and lead to faster formation of the hemiacetal.^[33]

Conclusion

Tandem catalysis under sustainable conditions is a topic of increasing interest for the one-pot synthesis of alkyl esters by alcohol oxidation. The efficient and selective aerobic oxidation of cinnamyl alcohol and *para*-substituted derivatives, such as *p*-chloro- and *p*-methoxy-cinnamyl alcohol, to the corresponding aldehydes has been successfully achieved under mild conditions, catalysed by AuNPs supported in a semi-crystalline nanoporous polymer matrix. Moreover, the cinnamyl alcohols are readily oxidised to alkyl cinnamates with high selectivity in presence of primary or secondary alkyl alcohols. The rate constants for the two reaction steps were measured in the temperature range 10–45 °C and the activation energy for cinnamyl alcohol oxidation and oxidative esterification of cinnamaldehyde with 1-butanol were calculated from the corresponding Arrhenius plots. It was shown that the first reaction step ($E_a = 57.8 \pm 11.5 \text{ kJ mol}^{-1}$), namely the oxidation of CA to cinnamaldehyde, is faster than the second reaction step ($E_a = 62.7 \pm 16.7 \text{ kJ mol}^{-1}$) that involves oxidation of the hemiacetal to the ester.

The kinetic studies allowed confirmation of the active role played by the nanoporous polymer matrix in the determination of both the activity and selectivity of the reaction. Actually, the kinetics of CA oxidation to cinnamaldehyde is first order with respect to the alcohol as result of fast migration of this reagent through the nanoporous polymer matrix; the second step is diffusion controlled for those alcohols, namely long-chain alkyl alcohols, which are not prone to permeate the polymer matrix. The latter reaction rates decrease as the steric hindrance of the alcohol increases (methanol ≈ ethanol ≈ 1-butanol > 2-propanol ≈ 1-hexanol > 1-octanol). On the contrary, the oxidative esterification of CA with 2-phenylethanol is pseudo-first order in both steps as a result of fast diffusion of the aromatic alcohols through the polystyrene matrix. These findings support the hypothesis that the oxidative esterification reaction occurs through two consecutive steps and not in a concerted way on the surface of the AuNPs.

Thus, the oxidative esterification reaction catalysed by AuNPs-sPSB was extended to *p*-substituted cin-

Table 5. Oxidative esterification of *p*-substituted cinnamyl alcohols with methanol and 1-butanol.

Entry ^[a]	R	Alkyl alcohol	Conversion ^[b] [%]	Products	Yield ^[c] [%]
1	–OMe	methanol	> 99	methyl <i>p</i> -methoxycinnamate <i>p</i> -methoxycinnamaldehyde 3-(<i>p</i> -methoxyphenyl)1-propanol	21 76 0.7
2	–OMe	1-butanol	> 99	butyl <i>p</i> -methoxycinnamate <i>p</i> -methoxycinnamaldehyde 3-(<i>p</i> -methoxyphenyl)1-propanol	6.2 91 0.7
3	–Cl	methanol	> 99	methyl <i>p</i> -chlorocinnamate <i>p</i> -chlorocinnamaldehyde	52 48
4	–Cl	1-butanol	> 99	butyl <i>p</i> -chlorocinnamate <i>p</i> -chlorocinnamaldehyde	26 74

[a] Reaction conditions: *p*-substituted CA (0.51 mmol), alkyl alcohol (5.1 mmol), AuNPs-sPSB (200 mg, Au = 2% w/w), O₂ (1 atm), H₂O/CHCl₃, (v/v = 1:1, total volume = 6 mL); 35 °C, KOH (3.06 mmol), 6 h, anisole as an internal standard (0.51 mmol). [b] Conversion of *p*-substituted CA determined by GC-MS analysis. [c] Determined by GC-MS.

namyl alcohols of potential pharmaceutical interest to support the general validity of the method.

Experimental Section

Materials and instrumentation

HAuCl₄·3H₂O (Sigma-Aldrich), sodium triethylborohydride (1.0 M in THF; Sigma-Aldrich), cinnamyl alcohol (97%; Fluka), cinnamaldehyde (98%; Carlo Erba), *p*-methoxycinnamaldehyde (96%; SAFC), *p*-chlorocinnamaldehyde (96%; Aldrich), methanol (HPLC grade; Sigma), ethanol (99.8%; Fluka), isopropyl alcohol (99.8%; Sigma-Aldrich), 1-butanol (98%; Labscan), 1-hexanol (98%; Sigma-Aldrich), 1-octanol (>99%; Sigma-Aldrich), sodium borohydride (98%; Sigma-Aldrich), hydrochloric acid (37%; Sigma-Aldrich), potassium hydroxide (85%; Sigma-Aldrich), anisole (99%; Sigma-Aldrich), water (HPLC grade; Pancreac), chloroform (HPLC grade; Romil), acetonitrile (HPLC grade; Sigma-Aldrich), ethyl acetate (>99.5%; Sigma-Aldrich), methyl ethyl ketone (99.5%; Carlo Erba) and cyclohexanone (>99.5%; Sigma-Aldrich) were used as received. *p*-Methoxycinnamyl alcohol and *p*-chlorocinnamyl alcohol were synthesised by reduction of the corresponding aldehydes by literature methods.^[34] Oxygen was supplied by Rivoira and used as received. Deuterated solvents were purchased from Euriso-Top or Sigma-Aldrich and used as received. The Au^{III} standard solution (Carlo Erba; 1.000 ± 0.002 g L⁻¹ in aqueous HCl solution, 2% w/w) for the AAS and ICP-OES measurements was used as received. The AuNPs-sPSB catalyst (Au = 2% w/w) was synthesised and characterised as previously reported.^[25,26]

NMR spectra were recorded with a Bruker AVANCE 400 spectrometer (400 MHz for ¹H and 100 MHz for ¹³C). WAXD patterns were obtained in reflection mode with an automatic Bruker D8 powder diffractometer and nickel-filtered Cu_{Kα} radiation. TEM analysis was carried out with a Tecnai 20 (FEI) microscope operating at 200 kV. The specimens for TEM analysis were sonicated in 2-propanol, then transferred (10 µL) onto a copper grid covered with a lacey carbon film supplied from Assing. The size-distribution analysis of the AuNPs was performed with the software Photoshop CS5 Extended. Atomic adsorption spectroscopy (AAS) and inductively coupled plasma optical emission spectrometry (ICP-OES) analysis of the AuNPs-sPSB catalyst were performed on a PerkinElmer AAAnalyst 100 spectrophotometer equipped with a Au hollow cathode lamp (PerkinElmer) and a PerkinElmer Optima 7000 DV spectrometer, respectively. DRIFTS measurements were performed with a Bruker Vertex 70 spectrometer. The catalyst solutions to be analysed were obtained as previously reported.^[25] GC analyses were performed with a GC-MS 7890A/5975C chromatograph from Agilent Technologies, equipped with a HP-Innowax column (polyethylene glycol, 30 m, 0.25 mm ID) or an Optima 17MS column (1:1 diphenylpolysiloxane/dimethylpolysiloxane, 30 m, 0.25 mm ID), a mass-selective detector and a FID detector.

General procedure for oxidation of cinnamyl alcohols catalysed by AuNPs-sPSB (Table 1, entry 2)

A round-bottom two-necked flask (50 mL) equipped with a magnetic stirrer bar was charged, in the order noted, with H₂O (3 mL), KOH (172 mg, 3.06 mmol), anisole (55 µL, 0.51 mmol), cinnamyl alcohol (66 µL, 0.51 mmol), CHCl₃ (3 mL) and catalyst (200 mg). The mixture was stirred at 35 °C under atmospheric pressure of O₂. Aliquots of the reaction mixture were sampled at the desired reaction time and treated with plenty of acetonitrile. The polymer was separated by filtration and the filtrate was analysed by GC-MS and

¹H NMR spectroscopy. At the end of the reaction, the polymer was coagulated in plenty of acetonitrile. The catalyst was recovered by filtration and the filtrate analysed by GC-MS.

General procedure for direct esterification of alcohols catalysed by AuNPs-sPSB (Table 2, entry 3)

A round-bottomed two-necked flask (50 mL) equipped with a magnetic stirrer bar was charged, in the order noted, with H₂O (3 mL), KOH (172 mg, 3.06 mmol), anisole (55 µL, 0.51 mmol), cinnamyl alcohol (66 µL, 0.51 mmol), 1-butanol (470 µL, 5.1 mmol), CHCl₃ (3 mL) and catalyst (200 mg). The mixture was stirred at 35 °C under atmospheric pressure of O₂. Aliquots of the reaction mixture were sampled at the desired reaction time and treated with plenty of acetonitrile. The polymer was separated by filtration and the filtrate was analysed by GC-MS and ¹H NMR spectroscopy. At the end of the reaction, the polymer was coagulated in plenty of acetonitrile. The catalyst was recovered by filtration and the filtrate analysed by GC-MS.

General procedure for direct esterification of cinnamaldehyde catalysed by AuNPs-sPSB (Table 4, entry 3)

A round-bottomed two-necked flask (50 mL) equipped with a magnetic stirrer bar was charged, in the order noted, with H₂O (3 mL), KOH (172 mg, 3.06 mmol), anisole (55 µL, 0.51 mmol), freshly distilled cinnamaldehyde (66 µL, 0.51 mmol), 1-butanol (470 µL, 5.1 mmol), CHCl₃ (3 mL) and catalyst (200 mg). The mixture was stirred at 35 °C under atmospheric pressure of O₂. Aliquots of the reaction mixture were sampled at the desired reaction time and treated with plenty of acetonitrile. The polymer was separated by filtration and the filtrate was analysed by GC-MS and ¹H NMR spectroscopy. At the end of reaction, the polymer was coagulated in plenty of acetonitrile. The catalyst was recovered by filtration and the filtrate analysed by GC-MS.

Acknowledgements

Financial support from Ministero dell'Istruzione dell'Università e della Ricerca (MIUR) (FARB-2012) and POR Campania FSE 2007-2013, "Sviluppo di reti di eccellenza tra Università - Centri di Ricerca - Imprese", Asse IV, "Materiali e strutture intelligenti" (MASTRI), CUP B25B09000010007. The authors thank Dr. Patrizia Iannece and Dr. Tonino Caruso for technical assistance with GC analysis and Dr. Maria Sarno for the TEM acquisitions.

Keywords: esterification • gold • nanoparticles • oxidation • supported catalysts

- [1] P. Sharma, *J. Chem. Pharm. Res.* **2011**, *3*, 403–423.
- [2] N. H. Nam, Y. J. You, Y. D. Kim, H. Hong, H. M. Kim, Y. Z. Ann, *Bioorg. Med. Chem. Lett.* **2001**, *11*, 1173.
- [3] S. Kumar, P. Arya, C. Mukherjee, B. K. Singh, N. Singh, V. S. Prasad, A. K. Ghose, *Biochemistry* **2005**, *44*, 15944.
- [4] A. Alexander, R. K. Choudhary, U.S. Patent No. 5527947, **1996**.
- [5] a) F. A. Carey, R. J. Sundberg, *Advanced Organic Chemistry 5th ed. Part B: Reactions and Synthesis*, Springer, Heidelberg, **2007**, p. 252; b) J. Otera, J. Nishikido, *Esterification: Methods, Reactions, and Applications*, Wiley-VCH, Weinheim, **2010**, pp. 3–157.
- [6] L. Shu, Y. Hongjun, *Eur. Chem. Bull.* **2013**, *2*, 76–77.
- [7] a) Y. Zhang, X. Cui, F. Shi, Y. Deng, *Chem. Rev.* **2012**, *112*, 2467–2505; b) M. Stratakis, H. Garcia, *Chem. Rev.* **2012**, *112*, 4469–4506; c) A. Corma,

- H. Garcia, *Chem. Soc. Rev.* **2008**, *37*, 2096–2126; d) S. B. Kalidindi, B. R. Jagirdar, *ChemSusChem* **2012**, *5*, 65–75; e) C. Della Pina, E. Falletta, M. Rossi, *Chem. Soc. Rev.* **2012**, *41*, 350–369; f) T. Mallat, A. Baiker, *Annu. Rev. Chem. Biomol. Eng.* **2012**, *3*, 11–28; g) J. M. Campelo, D. Luna, R. Luque, J. M. Marinas, A. A. Romero, *ChemSusChem* **2009**, *2*, 18–45; h) P. Zhao, N. Li, D. Astruc, *Coord. Chem. Rev.* **2013**, *257*, 638–665; i) M. Sankar, N. Dimitratos, P. J. Miedziak, P. P. Wells, C. J. Kiely, G. J. Hutchings, *Chem. Soc. Rev.* **2012**, *41*, 8099–8139; j) M. Chen, D. W. Goodman, *Chem. Soc. Rev.* **2008**, *37*, 1860–1870; k) *Modern Heterogeneous Oxidation Catalysis. Design, Reactions and Characterization* (Ed.: N. Mizuno), Wiley-VCH, Weinheim, **2009**.
- [8] M. Haruta, T. Kobayashi, H. Sano, N. Yamada, *Chem. Lett.* **1987**, *16*, 405–408.
- [9] L. Kesavan, R. Tiruvalam, M. H. A. Rahim, M. I. bin Saiman, D. I. Enache, R. L. Jenkins, N. Dimitratos, J. A. Lopez-Sanchez, S. H. Taylor, D. W. Knight, C. J. Kiely, G. J. Hutchings, *Science* **2011**, *331*, 195–199.
- [10] a) S. E. Davis, M. S. Ide, R. J. Davis, *Green Chem.* **2013**, *15*, 17–45; b) C. Parmeggiani, F. Cardona, *Green Chem.* **2012**, *14*, 547–564; c) T. Tsukuda, H. Tsunoyama, H. Sakurai, *Chem. Asian J.* **2011**, *6*, 736–748; d) C. P. Vinod, K. Wilson, A. F. Lee, *J. Chem. Technol. Biotechnol.* **2011**, *86*, 161–171; e) T. Mallat, A. Baiker, *Chem. Rev.* **2004**, *104*, 3037–3058; f) C. Lucchesi, T. Inasaki, H. Miyamura, R. Matsubara, S. Kobayashi, *Adv. Synth. Catal.* **2008**, *350*, 1996–2000.
- [11] J. Huang, T. Akita, J. Faye, T. Fujitani, T. Takei, M. Haruta, *Angew. Chem.* **2009**, *121*, 8002–8006; *Angew. Chem. Int. Ed.* **2009**, *48*, 7862–7866.
- [12] Y. Zhu, H. Qian, B. A. Drake, R. Jin, *Angew. Chem.* **2010**, *122*, 1317–1320; *Angew. Chem. Int. Ed.* **2010**, *49*, 1295–1298.
- [13] A. Corma, P. Serna, *Science* **2006**, *313*, 332–334.
- [14] a) J. K. Edwards, B. Solsona, E. N. Ntaijinja, A. F. Carley, A. A. Herzing, C. J. Kiely, G. J. Hutchings, *Science* **2009**, *323*, 1037–1041; b) S. J. Freakley, M. Piccinini, J. K. Edwards, E. N. Ntaijinja, J. A. Moulijn, G. J. Hutchings, *ACS Catal.* **2013**, *3*, 487–501.
- [15] M. Conte, C. J. Davies, D. J. Morgan, T. E. Davies, D. J. Elias, A. F. Carley, P. Johnston, G. J. Hutchings, *J. Catal.* **2013**, *297*, 128–136.
- [16] a) T. Ishida, M. Nagaoka, T. Akita, M. Haruta, *Chem. Eur. J.* **2008**, *14*, 8456–8460; b) R. Bernini, S. Cacchi, G. Fabrizi, S. Niembro, A. Prastaro, A. Shafir, A. Vallribera, *ChemSusChem* **2009**, *2*, 1036–1040; c) H. Miyamura, T. Yasukawa, S. Kobayashi, *Green Chem.* **2010**, *12*, 776–778; d) A. Wittstock, V. Zielasek, J. Biener, C. M. Friend, M. Bäumer, *Science* **2010**, *327*, 319–322; e) B. Xu, R. J. Madix, C. M. Friend, *J. Am. Chem. Soc.* **2010**, *132*, 16571–16580; f) B. Xu, J. Haubrich, C. G. Freyslag, R. J. Madix, C. M. Friend, *Chem. Sci.* **2010**, *1*, 310–314; g) F.-Z. Su, J. Ni, H. Sun, Y. Cao, H.-Y. He, K.-N. Fan, *Chem. Eur. J.* **2008**, *14*, 7131–7135; h) P. Liu, C. Li, E. J. M. Hensen, *Chem. Eur. J.* **2012**, *18*, 12122–12129; i) R. L. Oliveira, P. K. Kiyohara, L. M. Rossi, *Green Chem.* **2009**, *11*, 1366–1370; j) C. Marsden, E. Taarning, D. Hansen, L. Johansen, S. K. Klitgaard, K. Egeblad, C. H. Christensen, *Green Chem.* **2008**, *10*, 168–170; k) B. Xu, X. Liu, J. Haubrich, C. M. Friend, *Nat. Chem.* **2010**, *2*, 61–65.
- [17] J.-F. Soulé, H. Miyamura, S. Kobayashi, *J. Am. Chem. Soc.* **2011**, *133*, 18550–18553.
- [18] a) A. Abad, P. Concepcion, A. Corma, H. García, *Angew. Chem.* **2005**, *117*, 4134–4137; *Angew. Chem. Int. Ed.* **2005**, *44*, 4066–4069; b) A. Abad, A. Corma, H. García, *Chem. Eur. J.* **2008**, *14*, 212–222; c) Y. Pérez, C. Aprile, A. Corma, H. García, *Catal. Lett.* **2010**, *134*, 204–209.
- [19] C. L. Bianchi, P. Canton, N. Dimitratos, F. Porta, L. Prati, *Catal. Today* **2005**, *102*–*103*, 203–212.
- [20] a) H. Tsunoyama, H. Sakurai, Y. Negishi, T. Tsukuda, *J. Am. Chem. Soc.* **2005**, *127*, 9374–9375; b) H. Tsunoyama, N. Ichikuni, H. Sakurai, T. Tsukuda, *J. Am. Chem. Soc.* **2009**, *131*, 7086–7093.
- [21] D. Astruc, F. Lu, d J. R. Aranzaes, *Angew. Chem.* **2005**, *117*, 8062–8083; *Angew. Chem. Int. Ed.* **2005**, *44*, 7852–7872.
- [22] F. Shi, Q. Zhang, Y. Ma, Y. He, Y. Deng, *J. Am. Chem. Soc.* **2005**, *127*, 4182–4183.
- [23] a) H. Miyamura, R. Matsubara, Y. Miyazaki, S. Kobayashi, *Angew. Chem.* **2007**, *119*, 4229–4232; *Angew. Chem. Int. Ed.* **2007**, *46*, 4151–4154; b) M. Conte, H. Miyamura, S. Kobayashi, V. Chechik, *J. Am. Chem. Soc.* **2009**, *131*, 7189–7196.
- [24] a) C. Keresszegi, T. Bürgi, T. Mallat, A. Baiker, *J. Catal.* **2002**, *211*, 244–251; b) N. Dimitratos, A. Villa, D. Wang, F. Porta, D. Su, L. Prati, *J. Catal.* **2006**, *244*, 113–121; c) L. J. Durndell, C. M. A. Parlett, N. S. Hondow, K. Wilson, A. F. Lee, *Nanoscale* **2013**, *5*, 5412–5419.
- [25] A. Buonerba, C. Cuomo, S. Ortega Sánchez, P. Canton, A. Grassi, *Chem. Eur. J.* **2012**, *18*, 709–715.
- [26] a) A. Buonerba, M. Fienga, S. Milione, C. Cuomo, A. Grassi, A. Proto, C. Capacchione, *Macromolecules* **2013**, *46*, 8449–8457; b) A. Buonerba, V. Speranza, A. Grassi, *Macromolecules* **2013**, *46*, 778–784; c) A. Buonerba, C. Cuomo, V. Speranza, A. Grassi, *Macromolecules* **2010**, *43*, 367–374; d) C. Cuomo, M. C. Serra, M. Gonzalez Maupoey, A. Grassi, *Macromolecules* **2007**, *40*, 7089–7097; e) M. Caprio, M. C. Serra, D. E. Bowen, A. Grassi, *Macromolecules* **2002**, *35*, 9315–9322; f) N. Galdi, A. Buonerba, P. Oliva, L. Oliva, *Polym. Chem.* **2014**, DOI: 10.1039/C3PY01703F.
- [27] a) *Syndiotactic Polystyrene. Characterization, Processing, and Application* (Ed.: J. Schellenberg), John Wiley & Sons, Hoboken, New Jersey, **2010**; b) G. Milano, G. Guerra, *Prog. Mater. Sci.* **2009**, *54*, 68–88; c) E. B. Gowd, K. Tashiro, C. Ramesh, *Prog. Polym. Sci.* **2009**, *34*, 280–315; d) G. Guerra, C. Daniel, P. Rizzo, O. Tarallo, *J. Polym. Sci. Part B* **2012**, *50*, 305–322; e) M. Malanga, *Adv. Mater.* **2000**, *12*, 1869–1872; f) C. Capacchione, A. De Roma, A. Buonerba, V. Speranza, S. Milione, A. Grassi, *Macromol. Chem. Phys.* **2013**, *214*, 1990–1997; g) P. Rizzo, C. Daniel, A. De Girolamo Del Mauro, G. Guerra, *Chem. Mater.* **2007**, *19*, 3864–3866.
- [28] *Metal Nanoclusters in Catalysis and Material Science: The Issue of Size Control* (Eds.: B. Corain, G. Schmid, N. Toshima), Elsevier, Amsterdam, **2008**, pp. 131–132.
- [29] F. Kaneko, T. Tsuchida, *Polymer* **2013**, *54*, 760–765.
- [30] S. Bähn, S. Imm, L. Neubert, M. Zhang, H. Neumann, M. Beller, *ChemCatChem* **2011**, *3*, 1853–1864.
- [31] J. M. Mayer, *Acc. Chem. Res.* **2011**, *44*, 36–46.
- [32] C.-R. Chang, X.-F. Yang, B. Long, J. Li, *ACS Catal.* **2013**, *3*, 1693–1699.
- [33] a) R. Bruckner in *Advanced Organic Chemistry: Reaction Mechanisms*, Academic Press, San Diego, **2002**, p. 280; b) J. Clayden, N. Greeves, S. Warren, P. Wothers in *Organic Chemistry*, Oxford University Press, **2001**, pp. 143–147.
- [34] N. Usami, K. Kitahara, S. Ishikura, M. Nagano, S. Sakai, A. Hara, *Eur. J. Biochem.* **2001**, *268*, 5755–5763.

Received: October 3, 2013

Published online on March 18, 2014

CHEMISTRY

A European Journal

Supporting Information

© Copyright Wiley-VCH Verlag GmbH & Co. KGaA, 69451 Weinheim, 2014

Highly Efficient Direct Aerobic Oxidative Esterification of Cinnamyl Alcohol with Alkyl Alcohols Catalysed by Gold Nanoparticles Incarcerated in a Nanoporous Polymer Matrix: A Tool for Investigating the Role of the Polymer Host

Antonio Buonerba, Annarita Noschese, and Alfonso Grassi^{*[a]}

chem_201303880_sm_miscellaneous_information.pdf

Supporting Information

Highly Efficient Direct Aerobic Oxidative Esterification of Cinnamyl Alcohol with Alkyl Alcohols Catalyzed by Gold Nanoparticles Incarcerated in Nanoporous Polymer Matrix: a Tool for Investigating the Role of the Polymer Host

Antonio Buonerba,^[a] Annarita Noschese^[a] and Alfonso Grassi^{[a]}*

^[a] Dipartimento di Chimica e Biologia and NANOMATES Research Centre for NANOMaterials and nanoTEchnology at Salerno University,
Università degli Studi di Salerno,
Via Giovanni Paolo II, 84084 Fisciano (SA), Italy.

* E-mail: agrassi@unisa.it

TABLE OF CONTENTS

1. WAXD ANALYSIS OF AUNPs-sPSB CATALYST	3
<i>Figure S1.</i> WAXD pattern of the “as synthesized” AuNPs-sPSB catalyst.....	3
2. TEM ANALYSIS OF AUNPs-sPSB CATALYST	4
<i>Figure S2.</i> TEM micrograph of the “as synthesized “AuNPs-sPSB catalyst.....	4
<i>Figure S3.</i> SAED micrograph of the annealed AuNPs-sPSB catalyst (170 °C, 5 h) (Figure 2c)	5
3. DRIFT AND WAXD ANALYSIS OF AUNPs-sPSB CATALYST UNDER REACTION CONDITIONS IN WATER/CHLOROFORM SOLVENT MIXTURE.....	6
<i>Figure S4.</i> DRIFT (a) and WAXD (b) patterns of AuNPs-sPSB after an oxidation run. The patterns are diagnostic of the ε crystalline form of sPS. The characteristic assignments were labelled.....	6
4. REACTION PROFILES.....	7
<i>Figure S5.</i> Reaction profile of entry 1 of Table 1.....	7
<i>Table S1.</i> The course of reaction of entry 1 in Table 1.....	7
<i>Figure S6.</i> Reaction profile of entry 11 in Table 2.....	8
<i>Table S2.</i> The course of reaction in entry 11 in Table 2.....	8
<i>Figure S7.</i> Reaction profile of entry 13 of Table 2	9
<i>Table S3.</i> The course of reaction of entry 13 in Table 2	9
<i>Figure S8.</i> Reaction profile of entry 15 of Table 2	10
<i>Table S4.</i> The course of reaction of entry 15 in Table 2	10
<i>Figure S9.</i> Reaction profile of entry 23 in Table 4.....	11
<i>Table S5.</i> The course of reaction of entry 23 in Table 4	11
<i>Figure S10.</i> Reaction profile of entry 25 in Table 5.....	12
<i>Table S6.</i> The course of reaction of entry 25 in Table 5	12
<i>Figure S11.</i> Reaction profile of entry 26 in Table 5.....	13
<i>Table S7.</i> The course of reaction of entry 26 in Table 5	13
<i>Figure S12.</i> Reaction profile of entry 27 in Table 5.....	14
<i>Table S8.</i> The course of reaction of entry 27 in Table 5	14
<i>Figure S13.</i> Reaction profile of entry 28 of Table 5.....	15
<i>Table S9.</i> The course of reaction of entry 28 in Table 5	15
<i>Figure S14.</i> Arrhenius plot for CA oxidation to cinnamaldehyde in the temperature range of 10-45 °C	16
<i>Figure S15.</i> Arrhenius plot for the oxidative esterification of cinnamaldehyde with 1-butanol in the range of 10-45°C..	17

1. WAXD ANALYSIS OF AuNPs-sPSB CATALYST.

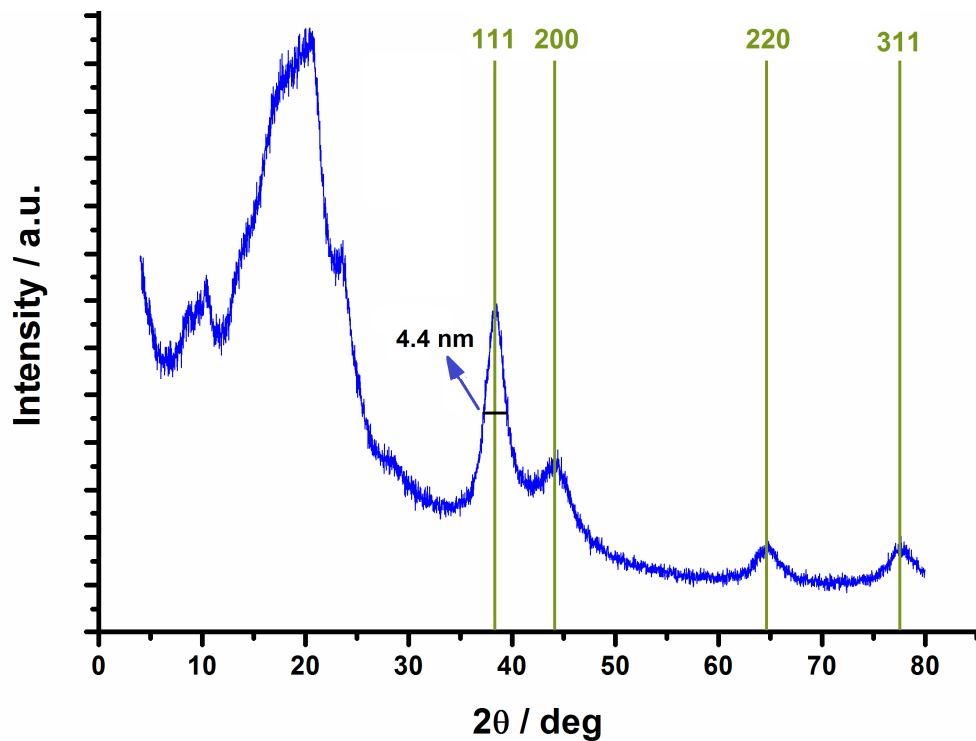


Figure S1. WAXD pattern of the “as synthesized” AuNPs-sPSB catalyst.

2. TEM ANALYSIS OF AUNPs-sPSB CATALYST.

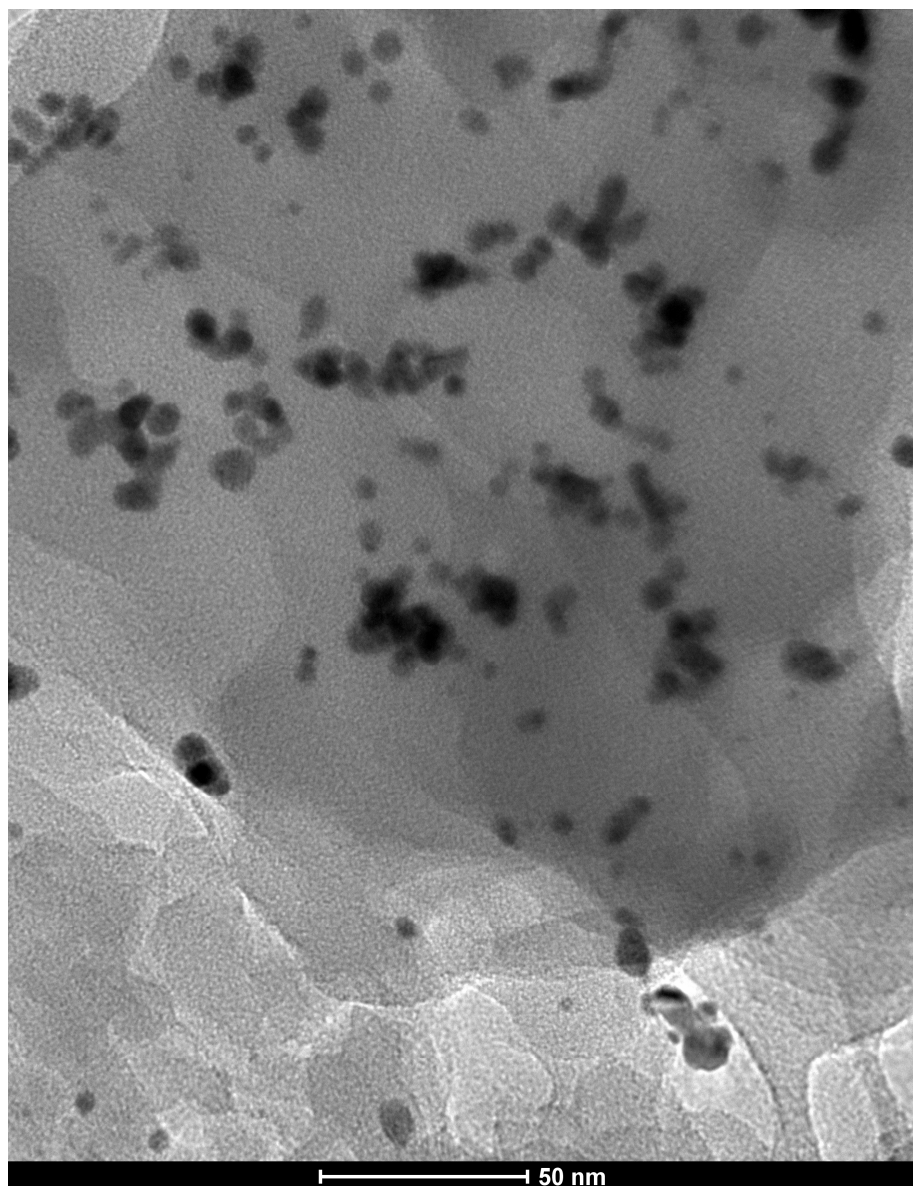


Figure S2. TEM micrograph of the “as synthesized” AuNPs-sPSB catalyst.

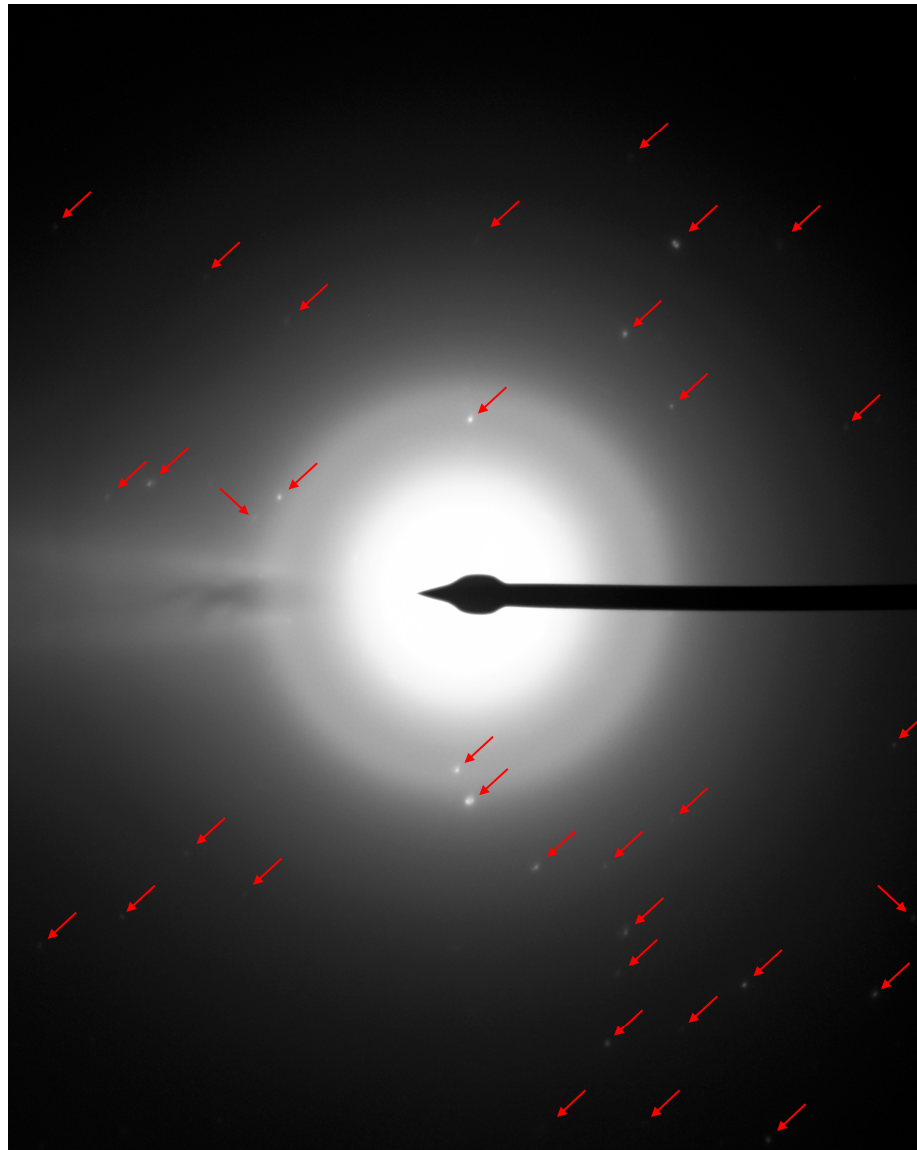


Figure S3. SAED micrograph of the annealed AuNPs-sPSB catalyst ($170\text{ }^{\circ}\text{C}$, 5 h) (Figure 2c).

3. DRIFT AND WAXD ANALYSIS OF AuNPs-sPSB CATALYST UNDER REACTION CONDITIONS IN WATER/CHLOROFORM SOLVENT MIXTURE.

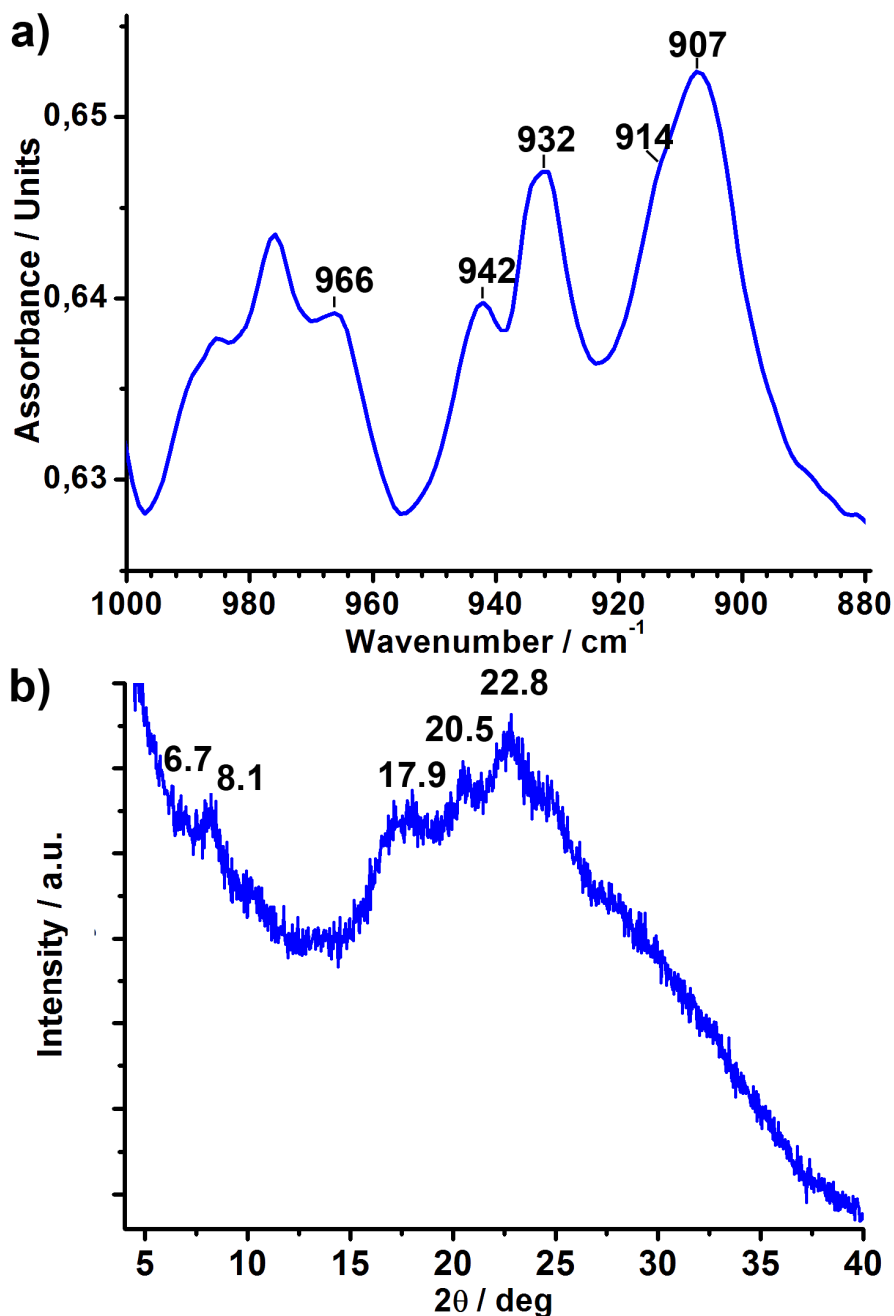


Figure S4. DRIFT (a) and WAXD (b) patterns of AuNPs-sPSB after an oxidation run. The patterns are diagnostic of the ϵ crystalline form of sPS. The characteristic assignments¹ were labelled.

¹ P. Rizzo, C. D'Aniello, A. De Girolamo Del Mauro, G. Guerra, *Macromolecules* **2007**, *40*, 9470-9474.

4. REACTION PROFILES.



Figure S5. Reaction profile of entry 1 of Table 1.

Table S1. The course of reaction of entry 1 in Table 1.

Time [h]	Cinnamyl alcohol [mol%]	Cinnamaldehyde [mol%]	3-Phenyl-1-propanol [mol%]
0	100	0.0	0.0
0.5	69.3	28.6	2.1
1	38.3	60.2	1.5
1.5	13.2	84.1	2.7
2	2.6	94.4	3.0
2.5	0.5	94.0	5.5
3	0.6	94.9	4.5
4	0.8	96.5	2.7
5	0.9	95.3	3.8
6	0.6	95.7	3.7
24	0.0	94.5	5.5

Reaction conditions: cinnamyl alcohol (0.51 mmol), AuNPs-sPSB (activated at 170 °C for 5 h, 200 mg; 2 wt%_{Au}), KOH (0.51 mmol), O₂ (1 atm), 35 °C, H₂O/CHCl₃ (v/v = 1:1, total volume 6 mL), anisole as an internal standard (0.51 mmol). Concentration values determined by GC-MS analysis.

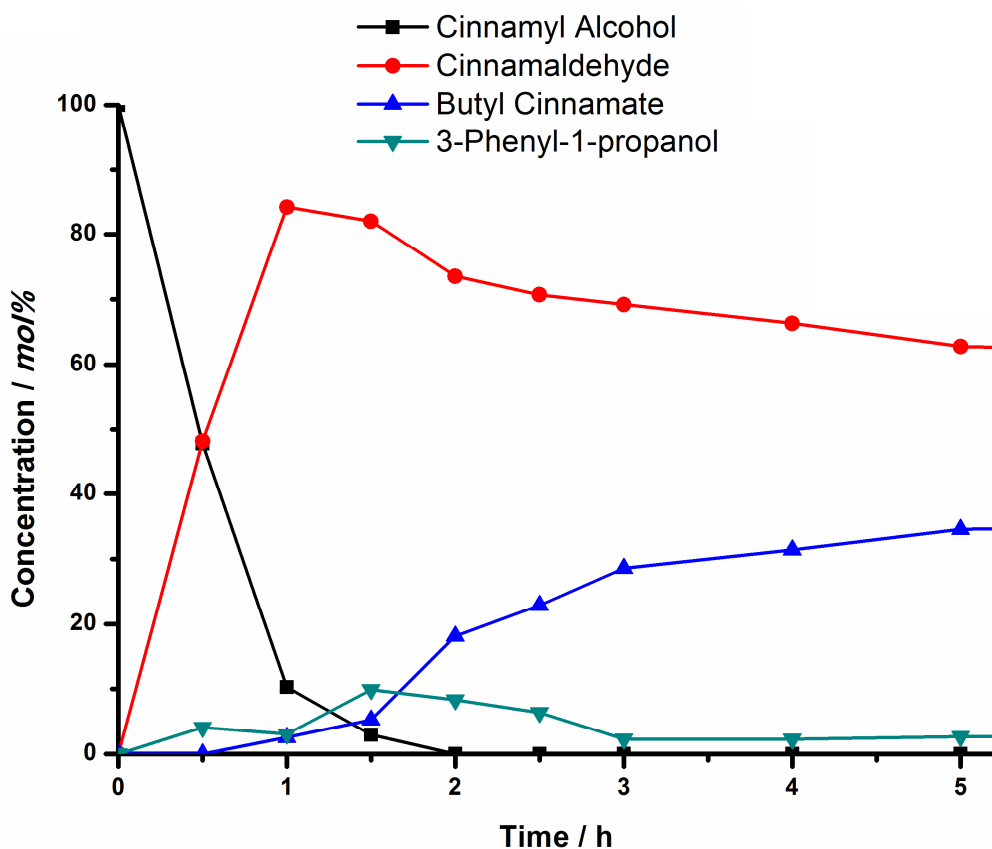


Figure S6. Reaction profile of entry 11 in Table 2.

Table S2. The course of reaction in entry 11 in Table 2.

Time [h]	Cinnamyl alcohol [mol%]	Cinnamaldehyde [mol%]	Butyl cinnamate [mol%]	3-Phenyl-1-propanol [mol%]
0	100	0.0	0.0	0.0
0.5	47.7	48.2	0.0	4.1
1	10.3	84.2	2.5	3.0
1.5	2.9	82.0	5.2	9.9
2	0.0	73.5	18.2	8.3
2.5	0.0	70.7	23.0	6.3
3	0.0	69.2	28.6	2.2
4	0.0	66.3	31.4	2.3
5	0.0	62.8	34.6	2.6
24	3.6	51.1	42.1	3.2

Reaction conditions: cinnamyl alcohol (0.51 mmol), 1-butanol (5.1 mmol) AuNPs-sPSB (activated at 170 °C for 5 h, 200 mg; 2 wt%_{Au}), KOH (0.51 mmol), O₂ (1 atm), 35 °C, H₂O/CHCl₃ (v/v = 1:1, total volume 6 mL), anisole as an internal standard (0.51 mmol). Concentration values determined by GC-MS analysis.

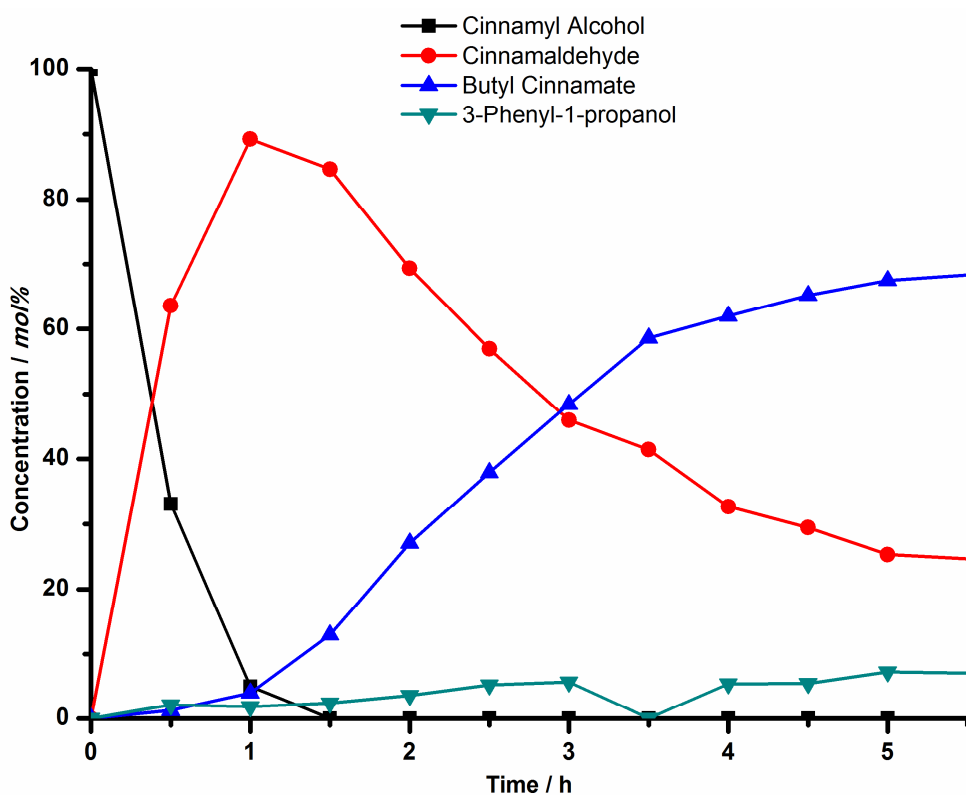


Figure S7. Reaction profile of entry 13 of Table 2.

Table S3. The course of reaction of entry 13 in Table 2.

Time [h]	Cinnamyl alcohol [mol%]	Cinnamaldehyde [mol%]	Butyl cinnamate [mol%]	3-Phenyl-1-propanol [mol%]
0	100	0.0	0.0	0.0
0.5	33.1	63.5	1.3	2.1
1	5.0	89.2	4.0	1.8
1.5	0.0	84.7	13.0	2.3
2	0.0	69.3	27.1	3.6
2.5	0.0	56.9	37.9	5.2
3	0.0	46.0	48.4	5.6
3.5	0.0	41.4	58.6	0.0
4	0.0	32.6	62.0	5.4
4.5	0.0	29.4	65.2	5.4
5	0.0	25.3	67.5	7.2
24	3.6	0.0	100	0.0

Reaction conditions: cinnamyl alcohol (0.51 mmol), 1-butanol (5.1 mmol) AuNPs-sPSB (activated at 170 °C for 5 h, 200 mg; 2 wt%_{Au}), KOH (3.06 mmol), O₂ (1 atm), 35 °C, H₂O/CHCl₃ (v/v = 1:1, total volume 6 mL), anisole as an internal standard (0.51 mmol). Concentration values determined by GC-MS analysis.

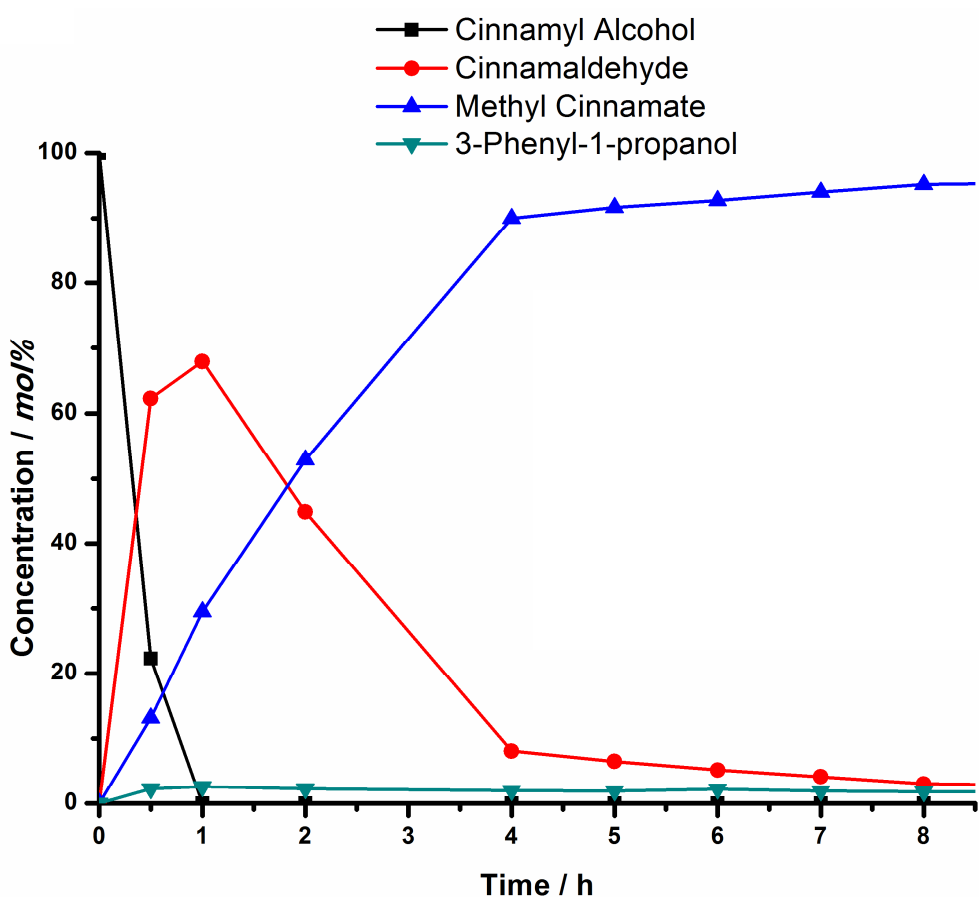


Figure S8. Reaction profile of entry 15 of Table 2.

Table S4. The course of reaction of entry 15 in Table 2.

Time [h]	Cinnamyl alcohol [mol%]	Cinnamaldehyde [mol%]	Methyl cinnamate [mol%]	3-Phenyl-1-propanol [mol%]
0	100	0.0	0.0	0.0
0.5	22.3	62.3	13.2	2.2
1	0.0	67.9	29.5	2.6
2	0.0	44.9	52.9	2.2
4	0.0	8.0	90.0	2.0
5	0.0	6.5	91.7	1.8
6	0.0	5.1	92.7	2.2
7	0.0	4.1	94.1	1.9
8	0.0	3.0	95.2	1.8
24	0.0	0.0	98.3	1.7

Reaction conditions: cinnamyl alcohol (0.51 mmol), methanol (5.1 mmol) AuNPs-sPSB (activated at 170 °C for 5 h, 200 mg; 2 wt%_{Au}), KOH (3.06 mmol), O₂ (1 atm), 35 °C, H₂O/CHCl₃ (v/v = 1:1, total volume 6 mL), anisole as an internal standard (0.51 mmol). Concentration values determined by GC-MS analysis.

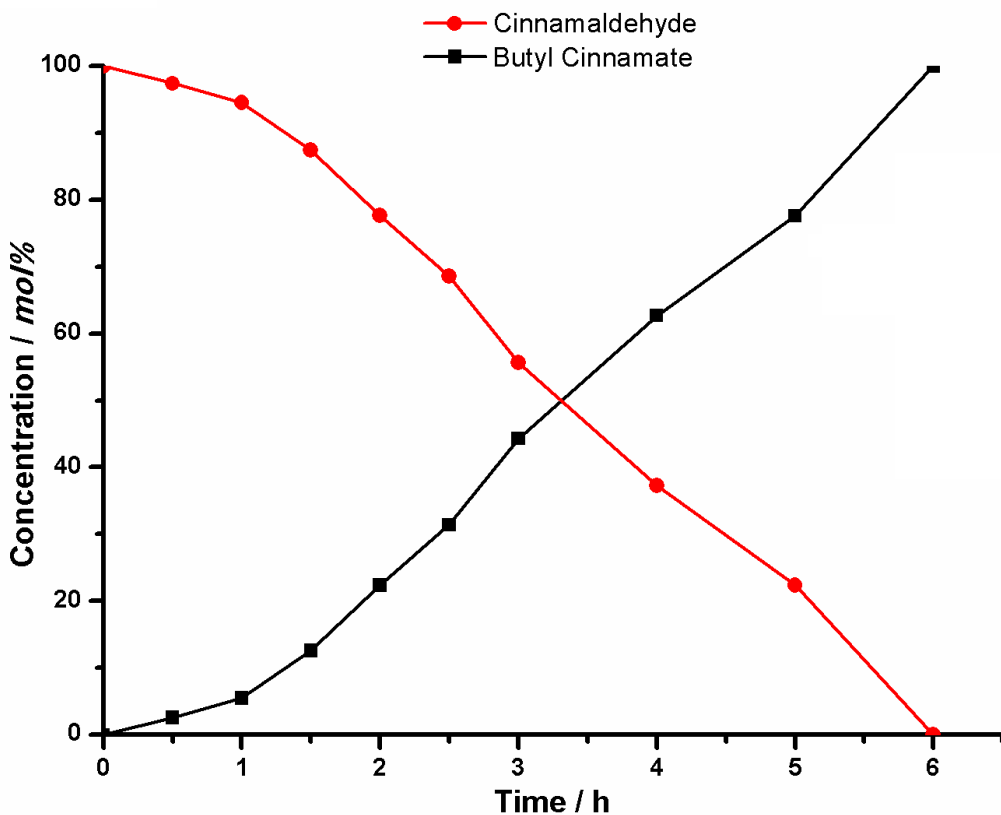


Figure S9. Reaction profile of entry 23 in Table 4.

Table S5. The course of reaction of entry 23 in Table 4.

Time [h]	Cinnamaldehyde [mol%]	Butyl cinnamate [mol%]
0	100	0.0
0.5	97.4	2.6
1	94.5	5.5
1.5	87.4	12.6
2	77.6	22.4
2.5	69.0	31.0
3	55.7	44.3
4	37.3	62.7
5	22.4	77.6
6	0.0	100

Reaction conditions: cinnamaldehyde (0.51 mmol), 1-butanol (5.1 mmol), AuNPs-sPSB (activated at 170 °C for 5 h, 200 mg; 2 wt%_{Au}), O₂ (1 atm), 35 °C, H₂O/CHCl₃ (v/v = 1:1, total volume 6 mL), KOH (3.06mmol), anisole as an internal standard (0.51 mmol). Concentration values determined by GC-MS analysis.

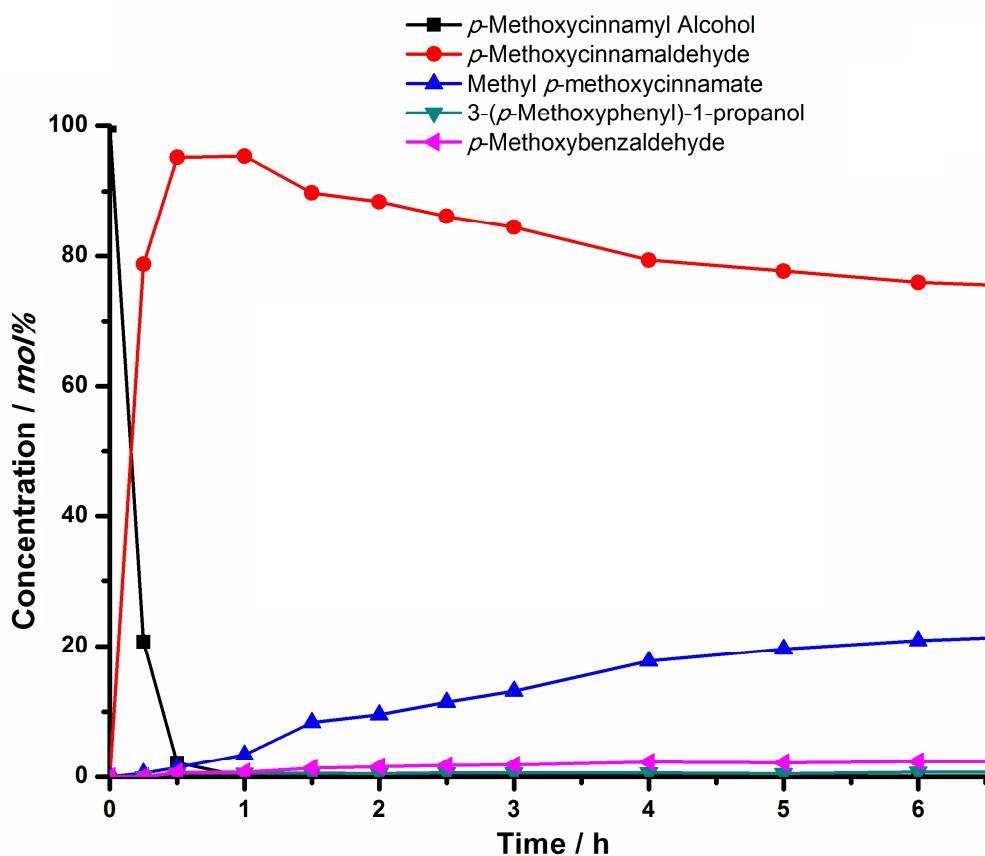


Figure S10. Reaction profile of entry 25 in Table 5.

Table S6. The course of reaction of entry 25 in Table 5.

Time [h]	p-Methoxy cinnamyl alcohol [mol%]	p-Methoxy cinnamaldehyde [mol%]	Methyl p-methoxy cinnamate [mol%]	3-(p-Methoxyphenyl) -1-propanol [mol%]
0	100	0.0	0	0.0
0.25	20.8	78.7	0.5	0.0
0.5	2.1	95.2	1.4	0.6
1	0.0	95.4	3.4	0.5
1.5	0.0	89.8	8.4	0.5
2	0.0	88.4	9.6	0.5
2.5	0.0	86.2	11.5	0.6
3	0.0	84.5	13.1	0.6
4	0.0	79.4	17.7	0.6
5	0.0	77.7	19.6	0.5
6	0.0	76.0	20.9	0.7
24	0.0	62.2	35.4	0.0

Reaction conditions: *p*-methoxycinnamyl alcohol (0.51 mmol), methanol (5.1 mmol), AuNPs-sPSB (activated at 170 °C for 5 h, 200 mg; 2 wt%_{Au}), O₂ (1 atm), H₂O/CHCl₃, (v/v = 1:1, total volume 6 mL), 35 °C, KOH (3.06 mmol), anisole as an internal standard (0.51 mmol). Concentration values determined by GC-MS analysis.

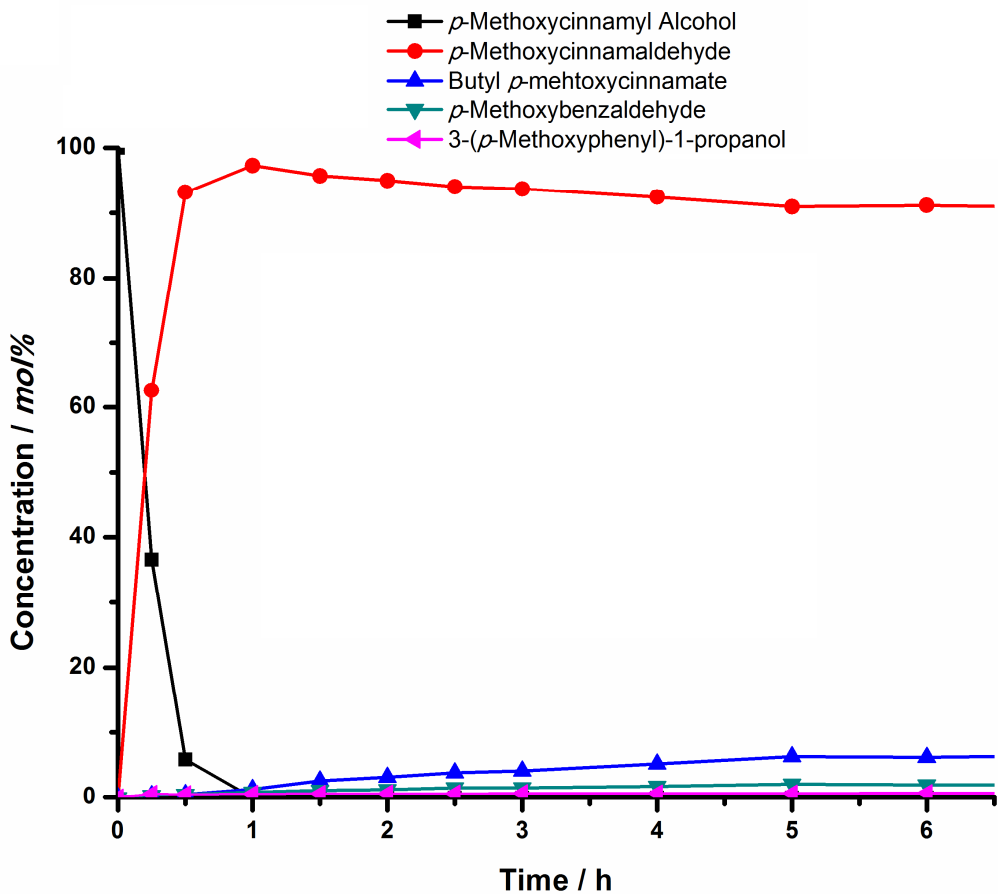


Figure S11. Reaction profile of entry 26 in Table 5.

Table S7. The course of reaction of entry 26 in Table 5.

Time [h]	<i>p</i> -Methoxy cinnamyl Alcohol [mol%]	<i>p</i> -Methoxy cinnamaldehyde [mol%]	Butyl <i>p</i> -methoxycinnamate [mol%]	<i>p</i> -Methoxy benzaldehyde [mol%]	3-(<i>p</i> -Methoxyphenyl)-1-propanol [mol%]
0	100	0.0	0.0	0.0	0.0
0.25	36.5	62.5	0.3	0.3	0.4
0.5	5.7	93.1	0.4	0.4	0.4
1	0.0	97.3	1.3	0.9	0.5
1.5	0.0	95.7	2.6	1.1	0.6
2	0.0	95.0	3.2	1.3	0.5
2.5	0.0	94.1	3.9	1.4	0.6
3	0.0	93.7	4.1	1.5	0.7
4	0.0	92.5	5.2	1.7	0.6
5	0.0	91.0	6.3	2.1	0.6
6	0.0	91.1	6.2	2.0	0.7
24	0.0	86.1	11.1	2.8	0.0

Reaction conditions: *p*-methoxycinnamyl alcohol (0.51 mmol), 1-butanol (5.1 mmol), AuNPs-sPSB (activated at 170 °C for 5 h, 200 mg; 2 wt%_{Au}), O₂ (1 atm), H₂O/CHCl₃, (v/v = 1:1, total volume 6 mL), 35 °C, KOH (3.06 mmol), anisole as an internal standard (0.51 mmol). Concentration values determined by GC-MS analysis.

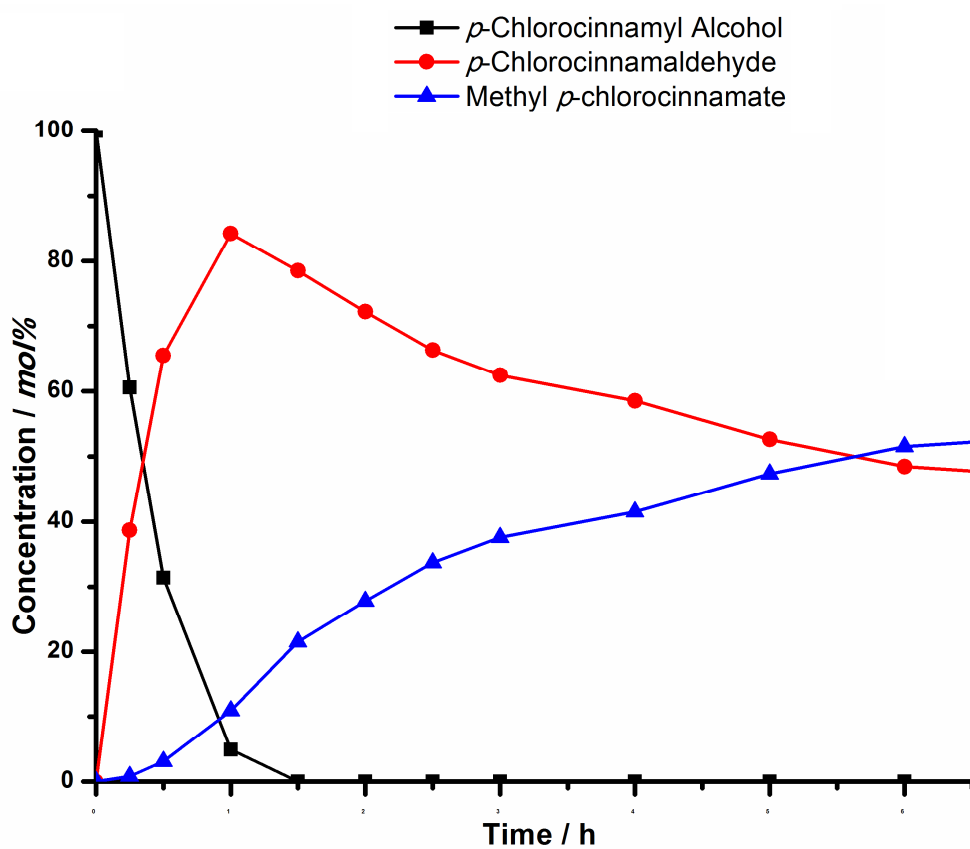


Figure S12. Reaction profile of entry 27 in Table 5.

Table S8. The course of reaction of entry 27 in Table 5.

Time [h]	<i>p</i> -Chlorocinnamyl alcohol [mol%]	<i>p</i> -Chlorocinnamaldehyde [mol%]	Methyl <i>p</i> -chlorocinnamate [mol%]
0	100	0.0	0.0
0.25	60.5	38.7	0.8
0.5	31.4	65.5	3.1
1	4.9	84.2	10.9
1.5	0.0	78.5	21.5
2	0.0	72.2	27.8
2.5	0.0	66.3	33.7
3	0.0	62.4	37.6
4	0.0	58.5	41.5
5	0.0	52.6	47.4
6	0.0	48.5	51.5
24	0.0	23.8	76.2

Reaction conditions: *p*-chlorocinnamyl alcohol (0.51 mmol), methanol (5.1 mmol), AuNPs-sPSB (activated at 170 °C for 5 h, 200 mg; 2 wt%_{Au}), O₂ (1 atm), H₂O/CHCl₃, (v/v = 1:1, total volume 6 mL), 35 °C, KOH (3.06 mmol), anisole as an internal standard (0.51 mmol). Concentration values determined by GC-MS analysis.

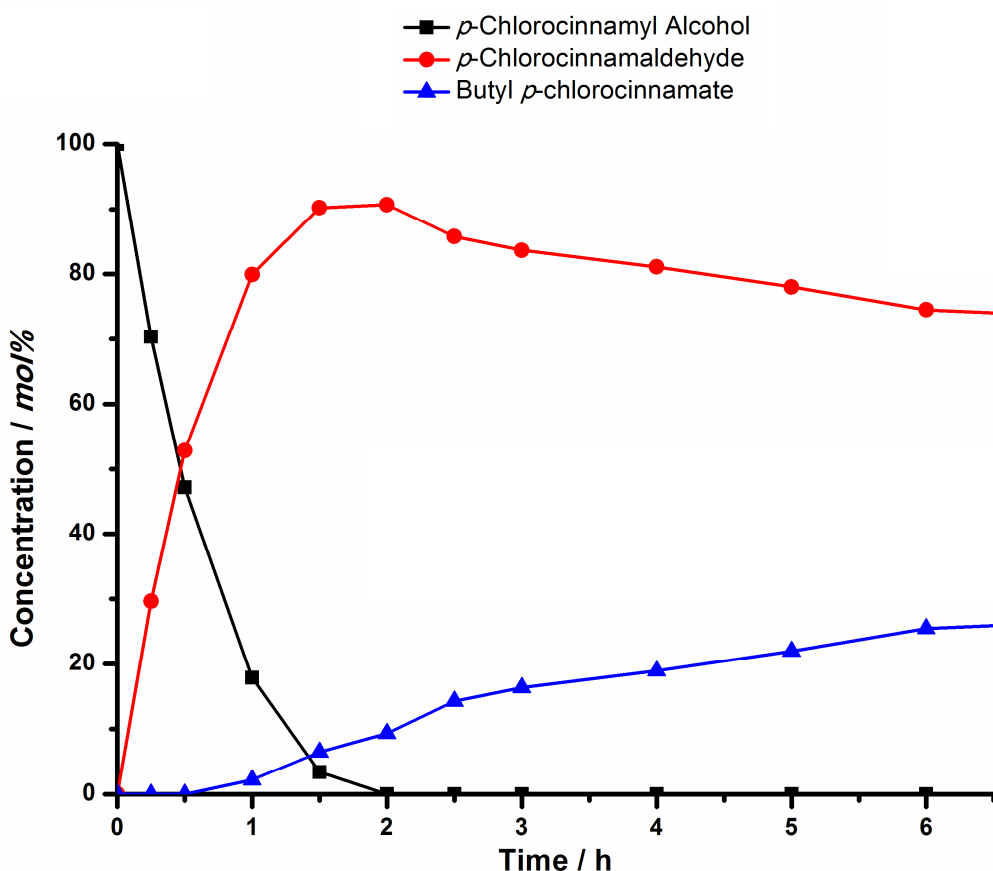


Figure S13. Reaction profile of entry 28 of Table 5.

Table S9. The course of reaction of entry 28 in Table 5.

Time [h]	<i>p</i> -Chlorocinnamyl alcohol [mol%]	<i>p</i> -Chlorocinnamaldehyde [mol%]	Butyl <i>p</i> -chlorocinnamate [mol%]
0	100	0.0	0.0
0.25	70.3	29.7	0.0
0.5	47.2	52.8	0.0
1	17.9	79.9	2.2
1.5	3.3	90.2	6.5
2	0.0	90.7	9.3
2.5	0.0	85.7	14.3
3	0.0	83.7	16.3
4	0.0	81.1	18.9
5	0.0	78.0	22.0
6	0.0	74.5	25.5
24	0.0	58.3	41.7

Reaction conditions: *p*-chlorocinnamyl alcohol (0.51 mmol), 1-butanol (5.1 mmol), AuNPs-sPSB (activated at 170 °C for 5 h, 200 mg; 2 wt%_{Au}), O₂ (1 atm), H₂O/CHCl₃, (v/v = 1:1, total volume 6 mL), 35 °C, KOH (3.06 mmol), anisole as an internal standard (0.51 mmol). Concentration values determined by GC-MS analysis.

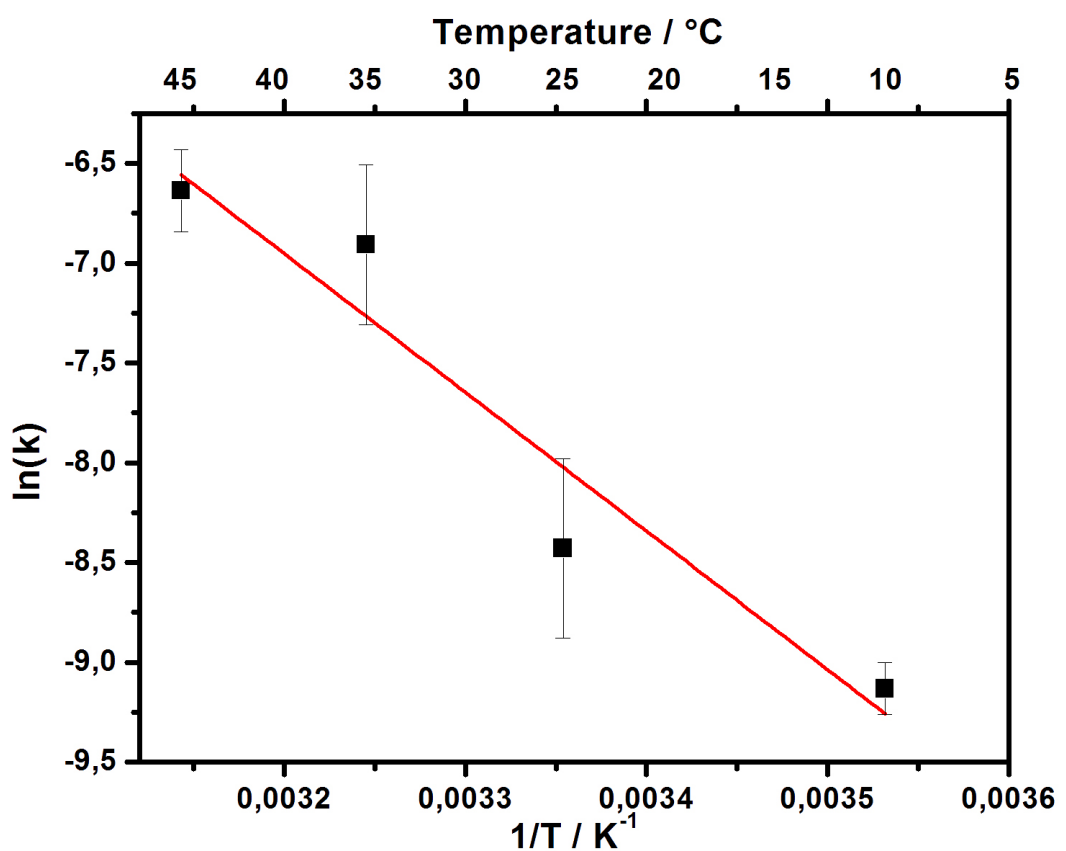


Figure S14. Arrhenius plot for CA oxidation to cinnamaldehyde in the temperature range of 10-45 °C.

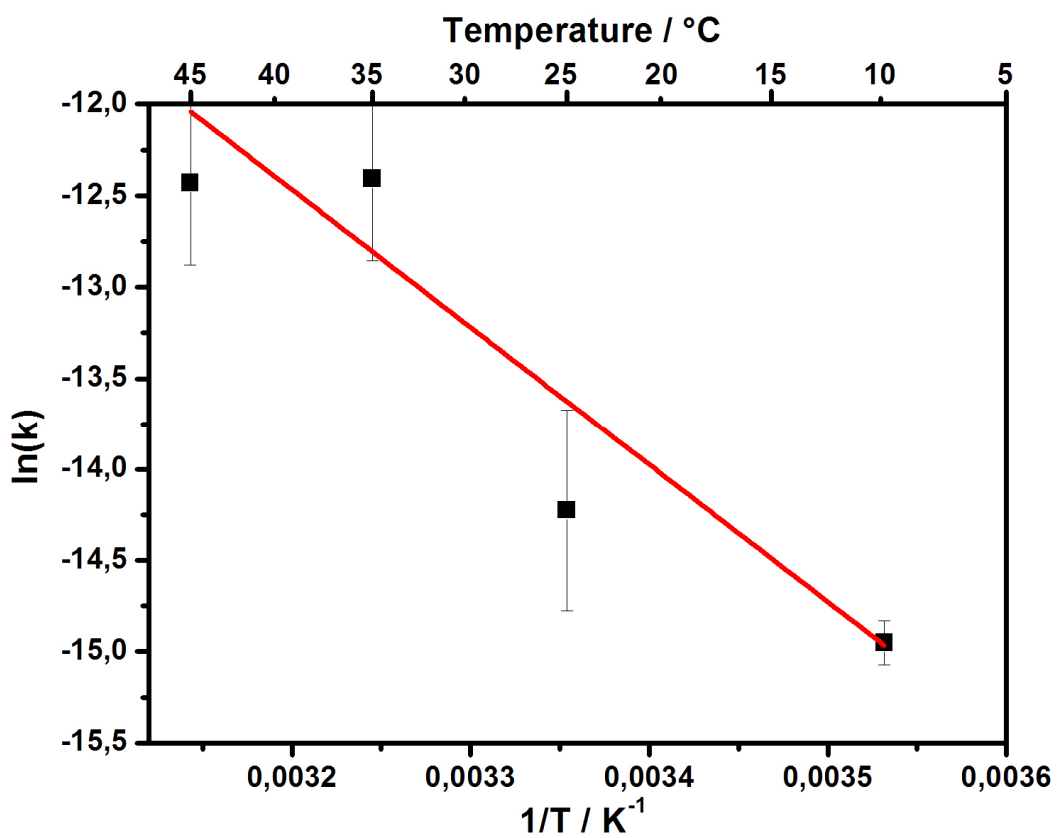


Figure S15. Arrhenius plot for the oxidative esterification of cinnamaldehyde with 1-butanol in the temperature range of 10-45°C.